AEDC-TR-73-140

AN EXPERIMENTAL INVESTIGATION OF AN ACOUSTIC METHOD FOR MEASURING GAS MASS FLOW

L. J. David and T. L. Giltinan
ARO, Inc.

September 1973

PROPULSION WIND TUNNEL FACILITY
ARNOLD ENGINEERING DEVELOPMENT CENTER
AIR FORCE SYSTEMS COMMAND
ARNOLD AIR FORCE STATION, TENNESSEE

NOTICES

When U. S. Government drawings specifications, or other data are used for any purpose other than a definitely related Government procurement operation, the Government thereby incurs no responsibility nor any obligation whatsoever, and the fact that the Government may have formulated, furnished, or in any way supplied the said drawings, specifications, or other data, is not to be regarded by implication or otherwise, or in any manner licensing the holder or any other person or corporation, or conveying any rights or permission to manufacture, use, or sell any patented invention that may in any way be related thereto.

Qualified users may obtain copies of this report from the Defense Documentation Center.

References to named commercial products in this report are not to be considered in any sense as an endorsement of the product by the United States Air Force or the Government.

AN EXPERIMENTAL INVESTIGATION OF AN ACOUSTIC METHOD FOR MEASURING GAS MASS FLOW

L. J. David and T. L. Giltinan
ARO, Inc.

FOREWORD

The work reported herein was done by the Arnold Engineering Development Center (AEDC), Air Force Systems Command (AFSC), Arnold Air Force Station, Tennessee under Program Element 65802F.

The results of research presented were obtained by ARO, Inc. (a subsidiary of Sverdrup & Parcel and Associates, Inc.), contract operator of AEDC. The work was done under ARO Project No. PW5213 from July 1971 to July 1972, and the manuscript was submitted for publication on January 10, 1973.

This technical report has been reviewed and is approved.

JOHN R. TAYLOR
Major, USAF
Chief, Research & Development Division
Directorate of Technology

ROBERT O. DIETZ
Director of Technology

ABSTRACT

Airflow through the test section of a 1- by 1-ft transonic wind tunnel under subsonic flow conditions was measured by an acoustic method to evaluate the feasibility of the method. The method was based on measuring the time of travel of an acoustic signal between a transmitter and a receiver which were located on opposite walls of the tunnel on a line perpendicular to the direction of airflow. Attempts to use pulsed ultrasonic transducers were not successful because of the characteristic time constant of a pulsed transducer and because of tunnel noise. An electrical discharge arc-gap transmitter was developed which emits a single pressure wave with an output intensity significantly greater than that of the tunnel noise. The velocity of the pressure wave is greater than the local speed of sound by an increment which arises from the overpressure caused by the arc discharge. Calibration of the wave velocity increment under quiescent conditions demonstrated very good repeatability. Correlation of mass flow obtained by the acoustic method with mass flow values obtained by considering the test section as a one-dimensional nozzle was excellent for a wave velocity increment value somewhat less than the calibrated value. The relationship between the quiescent wave velocity increment and the value required for good mass flow correlation was not found, and it remains to be defined.

CONTENTS

APPENDIXES

I. ILLUSTRATIONS

Figure

NOMENCLATURE

A	Area, ft^2
a	Speed of sound at static temperature, ft/sec
a_t	Speed of sound at total temperature, ft/sec
a_w	Wave velocity, ft/sec
$\bar{a}_w$	Average wave velocity, ft/sec
Δa	Wave velocity increment, ft/sec
$\overline{\Delta a}$	Average wave velocity increment, ft/sec
C	Capacitance, farads
D	Distance between transmitter and receiver, ft
d	Density, lb/ft^3
E	Voltage, volts
g	Acceleration of gravity, ft/sec^2
k	Specific heat ratio
m	Mass flow, lb/sec
P	Static pressure, psfa
P_t	Total pressure, psfa
Q	Electrical charge, joules
R	Gas constant, ft-lb/lb°R
S	Air path distance of signal, ft
T	Static temperature, °R
T_t	Total temperature, °R
t	Time, sec
Δt	Time of travel, sec
U	Signal velocity, ft/sec
$\overline{U}$	Average signal velocity, ft/sec
V	Flow velocity, ft/sec
$\overline{V}$	Average flow velocity, ft/sec

SECTION I
INTRODUCTION

The 16-ft Transonic Wind Tunnel of the Arnold Engineering Development Center (AEDC) has a potential capability for testing large turbofan engines under free-jet conditions. Evaluation of the internal performance of engines requires an accurate measurement of engine airflow, and methods for this measurement have not been available in the past. This report describes analytical and experimental work performed to evaluate the feasibility of a particular acoustic method for measuring engine airflow under free-jet conditions. It should be noted that the flight regime of interest is subsonic for turbofan engines, and that, in general, acoustic methods are not feasible for supersonic flows.

SECTION II
BACKGROUND

McShane* gives an excellent summary of the historical background of the development of acoustic methods for measuring fluid flow. In the period from 1919 to 1960, the three basic techniques were developed which govern all acoustic flow-measuring devices and systems. These techniques are referred to in the literature as (1) the time of travel difference, (2) Doppler phase shift, and (3) beam deflection. Early developments were hampered by the inadequacies of current state-of-the-art transducers and electronics, but in the 1950's, practical devices began to appear in the literature and on the market. Thereafter, many devices and systems were developed for both industrial and nonindustrial applications in the United States, in England, and in Russia. Those applications included velocity and flow measurements in liquids, gases, and slurries.

The axial cross-section of the inlet cowl of a turbofan engine includes a contracting section to a minimum area (throat), a short distance from the leading edge of the cowl, followed by an expanding section to the fan inlet. The three techniques of the preceding paragraph,

*McShane, J. L. "Ultrasonic Flowmeters." Scientific Paper 71-1C6-FLOME-P1, Westinghouse Research Laboratories, Pittsburg, Penna., August 13, 1971.

as applied to flow in ducts of constant cross-section, are dependent on upstream and downstream locations for the two transducers, transmitter and receiver, and therefore, they are not applicable to the inlet cowl of a turbofan engine. As described here, the technique investigated involved the direct measurement of the time of travel of the acoustic pulse from the transmitter to the receiver which were located in a plane normal to the flow. As applied to a turbofan engine, transducer pairs would be located at the throat station of the inlet cowl.

SECTION III
ANALYTICAL MODEL

The basic analytical model is illustrated by Fig. 1 (Appendix I) which represents a cross section through the axis of a cylindrical duct with flow from left to right. Assuming uniform flow, the velocity is equal and constant at all points in the flow. Similarly, pressure and temperature are constant and equal at all points in the flow.

At time zero, an acoustic pulse is emitted by a point source transmitter at B. Assuming this pulse is a single pressure wave, the wave expands spherically with time as it moves downstream with the flow, as indicated by the semicircles of increasing radius and displaced centers, 0. A point F on the surface of the wave will travel along the line B-G, and in some time interval after time zero, the point F is detected by a receiver at G. The velocity of F, designated as the signal velocity, is

$$U = D/\Delta t \tag{1}$$

where the time of travel, Δt, is measured by circuitry not shown in Fig. 1. The relationship between the flow velocity, the signal velocity, and the speed of sound is given by the vector diagram in the lower half of Fig. 1. Analytically,

$$V^2 = [a^2 - U^2] \tag{2}$$

The speed of sound is a function of temperature

$$a^2 = [gkRT] \tag{3}$$

In a uniform flow field, Eq. (3) applies to the static (free-stream) temperature. An accurate measure of static temperature is extremely difficult, but total temperature can be measured with comparative ease. It can be shown from the energy equation that

$$a^2 = a_t^2\left[1 - \frac{k-1}{2}\left(\frac{V}{a_t}\right)^2\right] \tag{4}$$

where

$$a_t^2 = [gkRT_t] \tag{5}$$

Combining Eqs. (2) and (5)

$$V^2 = \left[\frac{2}{k+1}\right]\left[a_t^2 - U^2\right] \tag{6}$$

or

$$V = \left(\left[\frac{2}{k+1}\right]\left[a_t^2 - U^2\right]\right)^{1/2} \tag{7}$$

Mass flow is equal to the product of volume flow and density

$$m = [(PAV)/(RT)] \tag{8}$$

Total and static temperatures can be equated by

$$T = T_t\left[1 - \left(\frac{k-1}{2}\right)\left(\frac{V}{a_t}\right)^2\right] \tag{9}$$

Combining Eqs. (8) and (9)

$$m = \frac{[PAV]}{[RT_t]\left[1 - \left(\frac{k-1}{2}\right)\left(\frac{V}{a_t}\right)^2\right]} \tag{10}$$

Combining (6) and (10)

$$m = \frac{\{a_t PA\}\left\{\left[\frac{2}{k+1}\right]\left[1 - \left(\frac{U}{a_t}\right)^2\right]\right\}^{1/2}}{\{RT_t\}\left\{1 - \left[\frac{k-1}{k-1}\right]\left[1 - \left(\frac{U}{a_t}\right)^2\right]\right\}} \tag{11}$$

Combining (1) and (11)

$$\dot{m} = \frac{\{a_t PA\}\left\{\left[\frac{2}{k+1}\right]\left[1 - \left(\frac{D}{\Delta t\, a_t}\right)^2\right]\right\}^{\frac{1}{2}}}{\{RT_t\}\left\{1 - \left[\frac{k-1}{k+1}\right]\left[1 - \left(\frac{D}{\Delta t\, a_t}\right)^2\right]\right\}} \tag{12}$$

Combining (5) and (12)

$$\dot{m} = \frac{\{PA\}\{gk\}^{\frac{1}{2}}\left\{\left[\frac{2}{k+1}\right]\left[1 - \left(\frac{D^2}{gkRT_t\Delta t^2}\right)\right]\right\}^{\frac{1}{2}}}{\{RT_t\}^{\frac{1}{2}}\left\{1 - \left[\frac{k-1}{k+1}\right]\left[1 - \left(\frac{D^2}{gkRT_t\Delta t^2}\right)\right]\right\}} \tag{13}$$

Equation (13) is a basic form of the mass flow equation. It is expressed in terms of the measured parameters which include area, diameter, static pressure, total temperature, and the time of flight of the acoustic pulse between the transmitter and the receiver, and it illustrates the fundamental aspects of the acoustic method. In practice, however, it may be more convenient to use other forms such as Eq. (10) in conjunction with Eqs. (7) and (1). The time of travel, Δt, in Eq. (13) is equal to the measured value corrected for circuit and wave shape effects as identified and defined in Appendix III.

The preceding development was based on two fundamental assumptions: (1) uniform flow and (2) the velocity of the pressure wave is equal in magnitude to the speed of sound at static temperature as given by Eq. (4). Nearly uniform flow occurs in direct-connect testing, in free-jet testing, and in flight testing of turbofan engines which are important areas of interest with regard to mass flow measurements. The velocity of the pressure wave is actually equal to the temperature dependent speed of sound plus an increment which is dependent on the magnitude of the overpressure; overpressure is defined here as the difference between the peak wave pressure and the ambient pressure of the medium. An example of this effect in another field is the shock wave standing off of the leading edge of the wing of an aircraft in supersonic flight. The shock wave is a pressure wave with a velocity equal

to the velocity of the aircraft. In some, if not in most applications, background noise will dictate an acoustic energy output by the transmitter of sufficient magnitude to include a significant overpressure effect. The corresponding analytical model with the wave velocity increment included is given in Appendix IV.

SECTION IV
TEST APPARATUS

The experimental work was conducted in the test section of the Aerodynamic Wind Tunnel (1T) of the Propulsion Wind Tunnel Facility. Tunnel 1T is a continuous flow nonreturn wind tunnel which can be operated at Mach numbers from 0.2 to 1.5, using variable nozzle contours above Mach 1.1. The test section is 1.0 ft square and 37.5 in. long. For the experimental work of this report, the nozzle was fixed on the sonic contour, and the walls were solid. Total pressure control is not available in Tunnel 1T, and the tunnel is operated at a stilling chamber pressure of about 2850 psfa with a ±5-percent variation depending on tunnel resistance and ambient atmospheric conditions. The stagnation temperature can be varied from 80 to 120°F above ambient atmospheric temperature.

The acoustic transmitter and receiver were installed on the centers of the floor and ceiling of the test section, respectively, as shown by the isometric illustration in Fig. 2. The line between the transmitter and the receiver was perpendicular to the floor and ceiling and, therefore, perpendicular to the flow. Mounting brackets on the backside of the walls positioned the transmitter and receiver so that the exposed surfaces were flush with the flow-side surfaces of the walls. Holes drilled in the walls for mounting screws and for penetration of the transmitter and receiver were filled and sanded to maintain the smooth flow surface.

Air mass flow through the test section was computed using the tunnel nozzle as the primary flow measuring device for comparison with the mass flows obtained by the acoustic method.

4.1 GENERAL

The circuitry of the system for acoustic mass flow measurement is illustrated by the line diagram of Fig. 3. Components of the basic system included the power supply, transmitter, counter, amplifier, filter, and receiver as shown. In operation, the transmitter was energized by a pulse from the power supply at time zero. Simultaneously, a signal pulse was sent to the counter which triggered the counter to start, and on arrival of the acoustic pulse, the output of the receiver triggered the counter to stop. Thus, the time of travel of the acoustic pulse between the transmitter and receiver was measured by the counter and then recorded from the counter display. A resistor-capacitor (R-C) filter followed the receiver to remove low-frequency tunnel noise components. The filtered receiver output was then amplified to increase the output voltage to the level required by the triggering circuit of the counter.

Two types of transmitters were evaluated: ultrasonic transducers and arc-gaps. Those transmitters, their characteristics, and differences in circuitry are described in the following sections.

4.2 TRANSDUCER TRANSMITTER

Ultrasonic transducers were evaluated initially. This type of transducer is basically a damped spring mass system. A stiff diaphragm on the end of a cylindrical barrel is excited by a piezoelectric crystal attached to the underside of the diaphragm. An oscillating voltage applied to the crystal causes the crystal to expand and contract, thus providing mechanical excitation for the diaphragm. Although excitation frequencies may be varied, the acoustic output is maximum when the excitation frequency is equal to the resonant frequency of the diaphragm.

A typical response of a transducer to a pulse input is shown by the oscillogram in Fig. 4. The lower trace is the electrical input which consisted of eight cycles at constant peak voltage and a frequency of 40 kHz. Amplitude is given by the ordinate, and elapsed time is given by the abscissa. The time scale in Fig. 4 is 200 μsec/cm with the distance between grid lines being 1 cm. Displacement to the right of the first cycle of the output with reference to the first cycle of the input corresponds to the time of travel of the acoustic output across the distance between the transmitter and receiver, approximately 1 ft in this

instance. Whereas the amplitude of the first cycle of the input pulse is maximum, the output amplitude increases with each cycle to a maximum on the fifteenth cycle. The time interval from the first to the fifteenth cycle represents the time constant of the transducer, the time for the output to reach maximum. The time constant is a characteristic of damped spring mass systems, and for the transducer of Fig. 4, it is approximately 380 μsec. The significance of the time constant with regard to time of travel measurements is discussed in the following.

The circuitry for the system with a transducer transmitter is shown in Fig. 5. The oscillator was used to generate a continuous oscillating voltage of a given frequency and amplitude which was directed to the tone burst generator. The tone burst generator acted as a switching device with regard to the input from the oscillator. The output of the generator could be set for a given number of cycles for each burst from one to 128 cycles with variation in multiples of two. Thus, the input trace in Fig. 4 is a burst of eight cycles. The burst repetition rate could be varied also to provide an adequate time interval between successive bursts. The generator output also includes a synchronizing pulse which coincides in time with the leading edge of the first cycle of the burst output. This synchronizing pulse was used as a trigger signal to start the counter. The signal burst from the tone burst generator was processed by the power amplifier which duplicated the burst in frequency and duration, but it increased the voltage to provide the desired power input to the transducer.

Other components in Fig. 5 which are common to Fig. 3 are as follows. The receiver included a mounting adapter which contained a preamplifier not shown in Figs. 3 and 5. This receiver was selected for the Aerodynamic Wind Tunnel (1T) installation because of its small size; the diameter of the microphone is 1/8 in. Also, its frequency response is very flat in the range from 0 to 100 kHz, which included the frequency region of interest. The filter included a 1000-ohm resistor and a 0.001-μf capacitor. The amplifier increased the voltage of the receiver output after filtering to the triggering level of the counter to stop the counter which measured the time of travel of the acoustic pulse as previously mentioned. An oscilloscope was connected in parallel with the counter as shown, and it was used to monitor transmission and reception of the acoustic signal for assistance in operation and maintenance of the system.

A listing of system components with identification by manufacturer and model number is given in Table I (Appendix II).

4.3 ARC-GAP TRANSMITTER

The arc-gap transmitter generates an acoustic pulse by an electrical arc across two exposed electrodes which are connected to a precharged capacitor. Energy stored in the capacitor is discharged in a single arc which has a very brief duration. The result is a miniature explosion, and the acoustic output is a single pressure wave which has an excellent signature for time of travel measurements.

An oscillogram of the first derivative of the arc-gap output is given by Fig. 6; the derivative appears instead of the amplitude because of the R-C filter. The spike on the left represents the rising side of the positive pressure half cycle of the pressure wave, and the second spike represents the rising side of the negative pressure half cycle. The time scale of Fig. 6 is 10 μsec/cm, and the trace shows that the equivalent time constant of the arc-gap is 2 μsec.

The arc-gap transmitter is illustrated schematically in Fig. 7. Two primary electrodes are connected to a charged capacitor, and the air-gap resistance of the electrodes prevents discharge of the capacitor. A trigger electrode is used to fire the arc-gap as follows. On receipt of an input signal, the trigger module acts as a switch to apply over 30,000 v to the trigger electrode. This applied voltage exceeds the breakdown voltage of the air-gap of the trigger to primary electrodes, and a weak arc jumps from the trigger electrode to the primary electrodes. This weak arc ionizes the air-gap of the primary electrodes, permitting the capacitor to discharge across the primary electrodes. Thus, the trigger electrode and trigger module collectively function as an instantaneous switch for discharging the high energy arc-gap on demand. The capacitor was recharged from a power supply as indicated.

The circuitry of the acoustic system with the arc-gap transmitter is given in Fig. 8. The arc-gap, arc-gap power supply and trigger module are shown as described in the preceding paragraph. The synchronizing pulse of the tone burst generator was used as the start signal for the trigger module and for the counter as shown. All other components are the same as described for the circuitry with the transducer of Fig. 5.

A listing of system components with identification by manufacturer and model number is given in Table II (Appendix II).

SECTION V
TEST RESULTS

Testing in Tunnel 1T was performed with continuously operating transducers, pulsed transducers, and arc-gap transmitters. Results and other aspects are discussed in the following.

5.1 CONTINUOUS TRANSDUCERS

Initial testing in Tunnel 1T was accomplished with a continuous ultrasonic transducer which was taken from a liquid-level-indicating system previously used in a cryogenic tank. The transducer had a time constant of 3000 μsec, and since the time of travel of the acoustic signal across the 1-ft dimension of the test section was less than 1000 μsec, the transducer could not be reasonably pulsed. The principal purpose of the tests was to obtain an early qualitative indication of the possibility of signal discrimination in the presence of tunnel noise.

Two transducers were installed in the test section as indicated in Fig. 2. One transducer was used as the transmitter and the other as the receiver. The output of the receiver was displayed by an oscilloscope which gave a visual comparison of signal and noise intensities. Signal-to-noise ratios of two or greater were observed at all tunnel Mach numbers up to 0.8.

A rough measure of mass flow rate was obtained with the continuous transducer from the phase shift of the acoustic signal. With no flow in the tunnel, the oscilloscope sweep rate was adjusted with regard to the frequency of the acoustic signal (40 kHz) to give a stationary wave form on the oscilloscope display. With flow then admitted to the test section, the display shifted (phase shift) by an amount proportional to the change in the time of travel of the acoustic signal from transmitter to receiver with reference to the time of travel with no flow. The change in time of travel is related to the flow velocity which was computed from the measured phase shift. Mass flow computed from that velocity measurement was comparable to mass flow computed from tunnel data within the accuracy of the phase shift measurement of approximately plus or minus 5 percent.

5.2 PULSED TRANSDUCER TRANSMITTER

Direct measurement of the time of flight is not feasible with a continuous signal, and for that purpose, a pulsed transducer with a very short time constant is required. The best transducer available from commercial sources had a time constant of 380 μsec. That transducer, previously mentioned with regard to Fig. 4, was used for the pulse tests in Tunnel 1T.

A typical oscillogram of the pulsed transducer is given by Fig. 9 for a tunnel Mach number of 0.3. The portion of the trace on the left of approximately constant amplitude, high solidity, and irregular boundary represents tunnel noise, and the oscillating trace on the right represents the transducer output which exceeds the noise. The electrical signal from the tone burst generator (see Fig. 5) was applied to the transmitter at time zero which corresponds to first vertical line on the left of the display grid. The time scale is 200 μsec/cm. Thus, Fig. 5 indicates a time of travel of approximately 850 μsec.

Accuracy requirements for time of travel measurement demand the timewise location of the first quarter of the first cycle of the acoustic pulse arriving at the receiver. Inspection of Fig. 9 shows that the first three or more cycles of the received pulse are masked by tunnel noise. Therefore, if the counter is started at time zero by the synchronizing pulse from the tone burst generator, as discussed previously, the triggering voltage for stopping the counter must be set at a value greater than the maximum voltage level of the noise component of the receiver output. Assuming the triggering voltage should be twice greater than the noise component voltage, Fig. 9 indicates that the measured time of travel will be greater than the true time of travel by an amount equal to the time interval of ten cycles. The transducer frequency of Fig. 9 was 40 kHz, and therefore, the measured time of travel would be in error by 250 μsec from that source alone. A correction could be applied if the number of cycles between the first cycle and the cycle on which triggering occurs is known. However, the location of the first cycle is unavailable, as previously mentioned. Also, the relatively small difference between peak amplitude values of successive cycles in the receiver output would permit triggering by one or the other of two adjacent cycles because of peak value variation from noise fluctuations. Therefore, the minimum error in measured time of travel of a pulsed transducer pulse would be two cycle periods. For a 40-kHz transducer, as was used to obtain the output shown in Fig. 9, that two-cycle uncertainty would be 50 μsec.

The two-cycle uncertainty defined by the preceding paragraph is inherent in transducers. It applies in any instance in which the peak amplitude of the first cycle is less than the amplitude of the noise component. Attempts to increase the peak amplitude of the first cycle of the transducer output by increasing the voltage input to the transducer by two orders of magnitude above its steady-state rating were not sufficient to overcome the problem. In all cases, the first cycle of the signal was masked by noise.

5.3 ARC-GAP TRANSMITTER

Development of the arc-gap transmitter was motivated by the two-cycle uncertainty of pulsed transducers as described in the preceding sub-section. The discharge of a capacitor across an arc-gap in the absence of inductive elements in the circuit occurs in a single burst and over a very small time interval. The resulting acoustic output is a one-cycle pulse with an equivalent time constant of small magnitude. The acoustic intensity of the output is dependent on the electrical energy discharged which can be varied as desired by the charging voltage and by the size of the capacitor.

5.3.1 Geometry

A photograph of the assembled arc-gap transmitter is shown in Fig. 10. The body of the assembly is cylindrical, and the material is lava. Lava is an insulator, and it was selected because it can be machined; other insulating materials could be used as well. The two primary electrodes are visible; the discharge heads are on the left, and the terminal ends are on the right. The arc discharges in a cavity between the heads. The dark lead in the foreground that penetrates the cylindrical surface is connected to the triggering electrode which is not visible.

Figure 11 is a cross-sectional view of the arc-gap showing the geometrical relationship of the trigger electrode to the primary electrodes. Although the sketch is not to scale, the small size of the trigger electrode relative to the primary electrodes is indicated. The trigger electrode was made from single strand 22-gage copper wire with the insulation removed from the exposed end. The gap dimension of the primary electrodes was 0.120 in.

5.3.2 Operation

The arc-gap and the capacitor were connected in a closed circuit as shown by Fig. 7. Power was fed into the circuit from a variable voltage transformer (not shown) through the diode. Thus, the capacitor could be charged to any desired voltage level by manually setting the output of the variable voltage transformer. The operating voltage range was between 1500 and 3000 v; the arc-gap would not discharge the capacitor below 1500 v, and the capacitor was limited to a maximum of 3000 v.

Discharge was initiated by a manual switch on the tone burst generator in the circuitry shown in Fig. 8. The synchronizing pulse output of the tone burst generator triggered the counter and the arc-gap as described in Section IV. Recharging of the capacitor began automatically on completion of discharge.

Energy stored in the capacitor varies directly with the square of the voltage and with the capacitance. Thus, the charge on the capacitor could be varied by a factor of 4.0 by varying the charging voltage between the lower and upper limits given previously. Two capacitors were available, one with a capacitance of 2.0 μf and the other with 25.0 μf. The acoustic output with the small capacitor was adequate to penetrate tunnel noise, and it was used for most of the tests in Tunnel 1T. The charging voltage was measured by a voltmeter which is not shown in Fig. 7.

5.3.3 Bench Tests

Discharge of the stored energy across the arc-gap is a miniature explosion in effect, and in the region of the arc, the peak pressure of the resulting pressure wave is greater than ambient pressure as previously mentioned. The velocity of the pressure wave is greater than the temperature dependent speed of sound by an increment which is dependent on the overpressure. This velocity, referred to hereafter as the wave velocity, may be written

$$a_w = a + \Delta a \tag{14}$$

where

$$a = [gkRT]^{1/2} \tag{15}$$

is the speed of sound and Δa is the incremental velocity resulting from the overpressure.

The magnitude of the velocity increment varies with the overpressure which decreases with increasing distance from the arc-gap, and the wave velocity, as given by Eq. (14), also decreases with increasing distance. Thus, the time of travel of the pressure wave to a point at some distance, x, from the arc-gap is a measure of the average wave velocity

$$\overline{a}_w = a + \overline{\Delta a}_w \tag{16}$$

where

$$\overline{\Delta a}_w = \frac{1}{x}\int_0^x \Delta a_w(x)dx \tag{17}$$

is the average value of the velocity increment.

The average wave velocity was measured at various distances from the arc-gap. Results are shown in Fig. 12 in which the average wave velocity is plotted against distance with electrical energy per discharge as a parameter. The discharged energy was equal to the stored energy

$$Q = E^2C \tag{18}$$

which has the units of joules when voltage is introduced in volts and capacitance in farads. Thus, with a capacitance of 2.0 μf, the discharge energy was varied from 2.25 joules to 9.0 joules by varying the charging voltage from 1500 to 3000 v. Figure 13 shows the average wave velocity for the arc-gap with a larger capacitor of 25.0 μf. Ambient temperature was 70°F at the time the data were taken, giving a speed of sound of 1128 ft/sec from Eq. (15) as indicated in Figs. 12 and 13. The value of the average velocity increment for a given discharge energy is equal to the difference between the corresponding curve and the given speed of sound, and it varies over a relatively wide range in the distance interval shown.

Measurements of the average wave velocity were repeatable within 0.5 percent for a given discharge energy level. That repeatability is a qualitative measure of the constancy of the efficiency of the arc-gap in converting electrical energy to acoustic energy at a given energy input. The results of Figs. 12 and 13 indicated that the efficiency

decreases with increasing input energy as evidenced by the relatively small change in the average velocity increment for large changes in the input energy, but at each input energy level, the data were repeatable. The significance of the repeatability is that it permits calibration of the arc-gap for the average wave velocity increment.

The previous remarks on calibration of the arc-gap for the average wave velocity increment were made primarily with reference to the data and results obtained. It should be noted however, that the efficiency of the arc-gap will be affected by the pressure and temperature of the medium. Obviously, the acoustic output would be zero in a vacuum, and a corresponding decrease in the output would occur with decreasing pressure of the medium as under altitude conditions. Therefore, calibrations of the arc-gap in the general case would include the density of the medium as a parameter in addition to the energy input.

An additional qualification on calibration of the arc-gap is related to the circuit elements which transfer energy from the capacitor to the arc-gap. One joule is equal to one watt-second and since the discharge occurs within a 5-μsec interval, as previously mentioned, the average discharge rate is equal roughly to 200 kw/joule stored in the capacitor. Thus, current flow through the circuit elements is quite high. For example, the discharge energy for the upper curve of Fig. 12 was 9.0 joules, with a charging voltage of 3000 v giving an average discharge rate of 1800 kw and an average current of 600 amp. It is evident that the resistance values of circuit elements can affect the acoustic output significantly by the dissipation of electrical energy in those elements. Also, the ionized resistance of the arc-gap is very small, which magnifies the influence of the transfer circuit resistance in that regard. Therefore, the calibration results in Figs. 12 and 13 represent the average wave velocity characteristics of the arc-gap and the energy transfer circuit elements as configured during the bench tests. Altering the transfer circuit with the same arc-gap would give different wave velocity values. The essence of the preceding discussion is that the acoustic output is dependent on the electrical energy delivered to the arc-gap which is equal to the stored energy minus circuit losses. This would not alter the value of a set of calibration curves, but it would limit the use of the curves to the specific transfer circuit and arc-gap configuration for which calibration data were taken.

5.3.4 Arc-Gap Transmitter Tests in Tunnel 1T

5.3.4.1 General

The arc-gap transmitter was installed in the solid wall test section of Tunnel 1T as illustrated in Fig. 2. The arc-gap was flush mounted in the floor, and the receiver was flush mounted in the ceiling. The capacitor was located in the plenum chamber underneath the floor within 1 ft of the arc-gap. Other components including the power supply, amplifier, filter, trigger module, and tone burst generator were located external to the plenum chamber.

Tests were performed by setting tunnel conditions for the desired Mach number. The arc-gap was fired by depressing a manual switch on the tone burst generator as previously mentioned. Time of travel as measured by the counter and tunnel pressure and temperature data were manually recorded. The charged condenser voltage was 3000 v for all test points. Condenser voltage was monitored by a voltmeter (not shown in Fig. 8) and a manually positioned variac (also not shown) was used on the input voltage to the power supply to set the condenser charging voltage.

5.3.4.2 Results

Results for a particular test run are shown in Fig. 14, in which mass flow is given versus test section Mach number. Mass flow was computed by the two methods of Appendix III, and the results are identified by the circular symbols for the acoustic method and the triangular symbols for the fluid flow method. Prior to the test run and immediately thereafter, the average wave velocity increment, $\overline{\Delta a}_w$ was measured with no flow in the test section. The condenser size was 2.0 μf and it was charged to 3000 v (9.0 joules). The measured value before and after the tests was 117 ft/sec, which is considerably higher than the corresponding value in Fig. 12 at a distance of 1.0 ft. The resistance of the transfer circuit was less in the tunnel installation than for the bench tests, and energy losses in the transfer circuit were less. Therefore, energy delivered to the arc-gap was greater, giving a higher wave-velocity increment.

Mass flow computed by the acoustic method and for the measured wave velocity increment of 117.0 ft/sec are given by the solid circular symbols. Those values are considerably higher than the fluid flow results, on the order of 18 percent at Mach 0.3 and 4 percent at Mach 0.6.

Using the data for the test point at Mach 0.28, a wave velocity increment was found analytically by trial and error which gave the same mass flow as the fluid flow method. That value of the wave velocity increment, 98 ft/sec, applied to the other test points in Fig. 14 gave mass flow values, open circular symbols, which correlate very well with the fluid flow results. The difference between the two values of the average wave velocity increment is obviously significant, and it is discussed in the following section.

An additional notation in Fig. 14 pertains to the direction of the arc with reference to the flow. The arc jumps from one electrode to the other, and its direction relative to flow direction is fixed by the rotational alignment of the electrodes. With regard to the results of Fig. 14, the direction of the arc in the tests was parallel to the direction of the flow in the test section of Tunnel 1T.

Figure 15 gives mass flow results for a test configuration which was the same as that for Fig. 14 with the exception that a 25.0-μf condenser was used. That change increased the stored energy from 9.0 to 112.5 joules, giving a larger wave velocity increment. The measured wave velocity increment was 188 ft/sec, which gave mass flow values greater than the corresponding values obtained by the fluid flow method. Good correlation was obtained with a velocity increment of 167 ft/sec, which was defined analytically by trial and error as described previously for Fig. 14.

The test configuration for the results in Fig. 16 was the same as that for the results in Fig. 14; the small condenser was reinstalled. The measured wave velocity increment was 107 ft/sec, and the required value for flow correlation was 92 ft/sec, as given in Fig. 16. The results in Figs. 14 and 16 are comparable with no significant differences being apparent. The smaller value of the measured wave velocity increment of Fig. 16 was probably caused by an increase in the electrical resistance of the transfer circuit. Exchanging the large and small condensers involved breaking the circuit at the condenser terminals. The terminal connections were made by pressure-type connectors, and the contact resistance can vary significantly as the connectors are broken and remade with particular regard to the large instantaneous magnitude of the current pulse.

The test configuration for the results in Fig. 17 was the same as that used to obtain the results given in Figs. 14 and 16 except that the arc-gap was rotated so that the arc direction was perpendicular to the

flow. Rotation of the arc-gap was accomplished without breaking the transfer circuit. The measured wave velocity increment was 107 ft/sec, the same as in Fig. 16. An assumed velocity increment of 92 ft/sec was used, as in Fig. 16, to compute the mass flow for the open circular symbols. Those mass flow values are slightly higher than the corresponding fluid flow values, whereas in Fig. 16 the mass flow values from the acoustic method are essentially equal to those from the fluid flow method. That difference suggests that the wave velocity increment may be slightly higher when the flow is in the direction perpendicular to the arc.

SECTION VI
DISCUSSION

6.1 WAVE VELOCITY

The wave velocity, has been shown to be equal to the speed of sound plus an increment dependent on the initial strength of the signal and the distance from the source. In application, the wave velocity increment is not a measurable quantity, and a prior calibration will be required such as that given in Figs. 12 and 13.

Repeatability of the data was very good for Figs. 12 and 13, which implies that calibration data can be obtained to a high degree of accuracy. Average wave velocities given in Figs. 12 and 13 follow a simple power function. For a given condenser input energy

$$\bar{a}_w = a + \overline{\Delta a}_{w1}(x)^{-2/3} \qquad (19) \qquad (19)$$

where

x = distance from source in feet

$\overline{\Delta a}_{w1}$ = average wave velocity increment at a distance of 1.0 ft

Values computed by Eq. (19) deviate from the curve values by less than 0.5 percent. It should be noted, however, that Eq. (19) does not apply at distances very close to the source. As the variable x approaches zero, the wave velocity would increase to infinity, which is impossible.

The density of the medium will affect the wave velocity increment. Attenuation in air increases with decreasing density. Also, the acoustic output for a given electrical input energy will decrease, and this implies a corresponding decrease in the initial value of the velocity increment. Therefore, calibration would be required under the same density conditions which would occur in use, and the complete calibration may include the pressure and temperature of the medium as parameters. The results in Figs. 12 and 13 were obtained under ground level ambient conditions, and project resources did not permit an investigation of density effects.

The use of the word "calibration" in the preceding remarks is perhaps misleading. Calibration normally refers to a comparison of the measure of a value by an instrument with the measure of the same value by a standard. Calibration for the average velocity, as described above, does not involve a standard, and it requires the velocity measurement by the instrument at a known distance under quiescent conditions. The variation of the wave velocity is a function of distance and the properties of the medium independently of the instrument. Therefore, calibration could be accomplished in place at any time that quiescent conditions exist or can be established. This will be true of course only if a definite relationship can be developed for the variation with density as with distance.

6.2 MASS FLOW

Test results show that the accuracy of the acoustic method in measuring mass flow will depend in large part on the accuracy to which the variation of the wave velocity increment can be predicted. Calibration of the wave velocity increment, as discussed in the preceding subsection, will be essential, but calibration data will only provide the basis on which to account for the variation of the velocity increment.

Correlation of the mass flow values computed with a wave velocity increment determined from Eq. (IV-25) and the data of a test point (open circular symbols in Figs. 14 through 17) with mass flows computed by the fluid flow method is very good, as previously mentioned. Using the calibrated wave velocity increment for a distance of 1.0 ft gave considerably higher mass flow values (the solid circular symbols) but the difference between the mass flows given by the solid and open circular symbols is essentially the same in Figs. 14 through 17. Since

the wave velocity increment values differ except in Figs. 16 and 17, the flow correspondence suggests the existence of an explicit relationship between the calibrated velocity increment, and the velocity increment required in Eq. (IV-25) for the correct mass flow.

The vector diagram of Fig. 1 gives the relationship between the acoustic velocity, a, the flow velocity, V, and the signal velocity, U, for the case in which the wave velocity increment is zero. A similar diagram can be drawn with the velocity increment present by replacing the acoustic velocity, a, with the average wave velocity, $\bar{a}_w$, and the signal velocity, U, with the average signal velocity, $\overline{U}$. Considering the vector diagram applied at the receiver, the distance traveled by the pressure wave to the receiver from the transmitter is

$$S = \frac{D}{\cos\theta} \tag{20}$$

Combining Eqs. (19) and (20), the average wave velocity increment at the receiver is then

$$\overline{\Delta a}_w = \overline{\Delta a}_{w1} \left(\frac{\cos\theta}{D}\right)^{2/3} \tag{21}$$

Using Eq. (21) to obtain the velocity increment for use in Eq. (IV-25) does not resolve the discrepancy. With reference to the calibrated velocity increment at a distance of 1.0 ft, $\Delta\bar{a}_1$, Fig. 14, for example, requires a reduction of 19 percent in the average wave velocity from 117 ft/sec to 98 ft/sec for good correlation. The corresponding reduction by Eq. (21) is on the order of 3 percent at a Mach number of 0.3 and 14 percent at 0.6.

Although Eq. (21) may be involved in the application of calibration data to mass flow computations by Eq. (IV-25), it does not stand alone. The complete relationship, was not determined, and it remains as an unresolved question for priority assessment in following efforts.

6.3 NONUNIFORM FLOW

Any flow situation in which the velocity is not equal and constant at all points in a plane perpendicular to the direction of flow is nonuniform. The principal output of the acoustic system is the average velocity along the line between the transmitter and receiver, but an area weighted average velocity is required to compute mass flow. By

definition, line and area weighted average values are the same in uniform flow. In nonuniform flow, line and area average velocities are not equal, and the system as described herein must be altered. Considering the circular cross section of the duct at the measuring station, line average velocities along a number of chords on both sides of the diameter would provide sufficient information with which to characterize the flow and from which the area weighted average flow velocity could be extracted. That approach was beyond the scope of this report, and it represents a second priority area for investigation in continuing efforts.

6.4 UPPER FLOW VELOCITY LIMIT

Inspection of Fig. 1 shows that the method of this report is limited to flow Mach numbers less than unity. As the flow velocity, V, approaches the local speed of sound, a, the Mach angle, θ, approaches 90 deg, and the signal velocity, U, approaches zero. Therefore, the time of travel increases to infinity for Mach numbers of unity or greater. With regard to the time of travel, the upper Mach number limit may be very close to unity. In a 10-ft-diam duct, for example, the time of travel for a Mach number of 0.99 would be approximately 0.08 sec, which would support an ample sampling rate. However, the effective path length in the moving airstream increases with Mach number, and attenuation of the signal strength increases with the square of the path length. Therefore, the upper limit will probably be determined by the background noise of each installation with regard to the initial signal strength at zero flow and attenuation with increasing Mach number. At a Mach number of 0.99, for example, the attenuation is approximately 17 db.

The upper limit also appears in Eq. (III-3), which defines the influence of Mach number on the rise time of the received acoustic pulse. At zero Mach number, the rise time of the pulse was 2.0 μsec as given in Appendix III. At unity Mach number, the rise time becomes infinite, which tends to imply the invalidity of Eq. (III-3). However, the equation is valid below unity Mach number, and at 0.99, for example, the rise time would be approximately 100 μsec. Thus, Eq. (III-3) is valid within the operating range of the method as described in the preceding paragraph.

SECTION VII
CONCLUDING REMARKS

An acoustic method for measuring gas mass flow was investigated in Tunnel 1T under nearly uniform flow conditions. The fundamental aspects of the method included the direct measurement of the time of travel of an acoustic pulse between a transmitter and a receiver which were installed in opposite walls of the wind tunnel and on a line perpendicular to the flow. Acoustic transducers were found to be inadequate because of tunnel noise which masked the leading edge of the received pulse. An electrical discharge transmitter was developed which emits a single cycle pulse with a very steep leading edge, and which provides sufficient acoustic power to penetrate tunnel noise. The velocity of the output pressure wave includes an increment, wave velocity increment, which decreases in magnitude with distance traveled from the source. This velocity increment is caused by the overpressure of the transmitter output, and although it was encountered with the electrical discharge transmitter, it can occur also with any type of transmitter. The effect of the velocity increment may be nil in those cases where low level background noise permits low power transmitters, but in the general case, it is a significant factor. Values for the velocity increment measured under quiescent conditions gave large errors in the computed mass flow, and methods and techniques to account for this variable remain to be determined. Thus, the feasibility of the method was not well established. However, excellent correlation obtained with arbitrary values for the velocity increment suggests that such methods and techniques may in fact exist although as yet undetermined. Nonuniform flow conditions were not investigated.

APPENDIXES

I. ILLUSTRATIONS
II. TABLES
III. TIME OF TRAVEL MEASUREMENT
IV. ANALYTICAL PROCEDURES
V. ERROR ANALYSIS

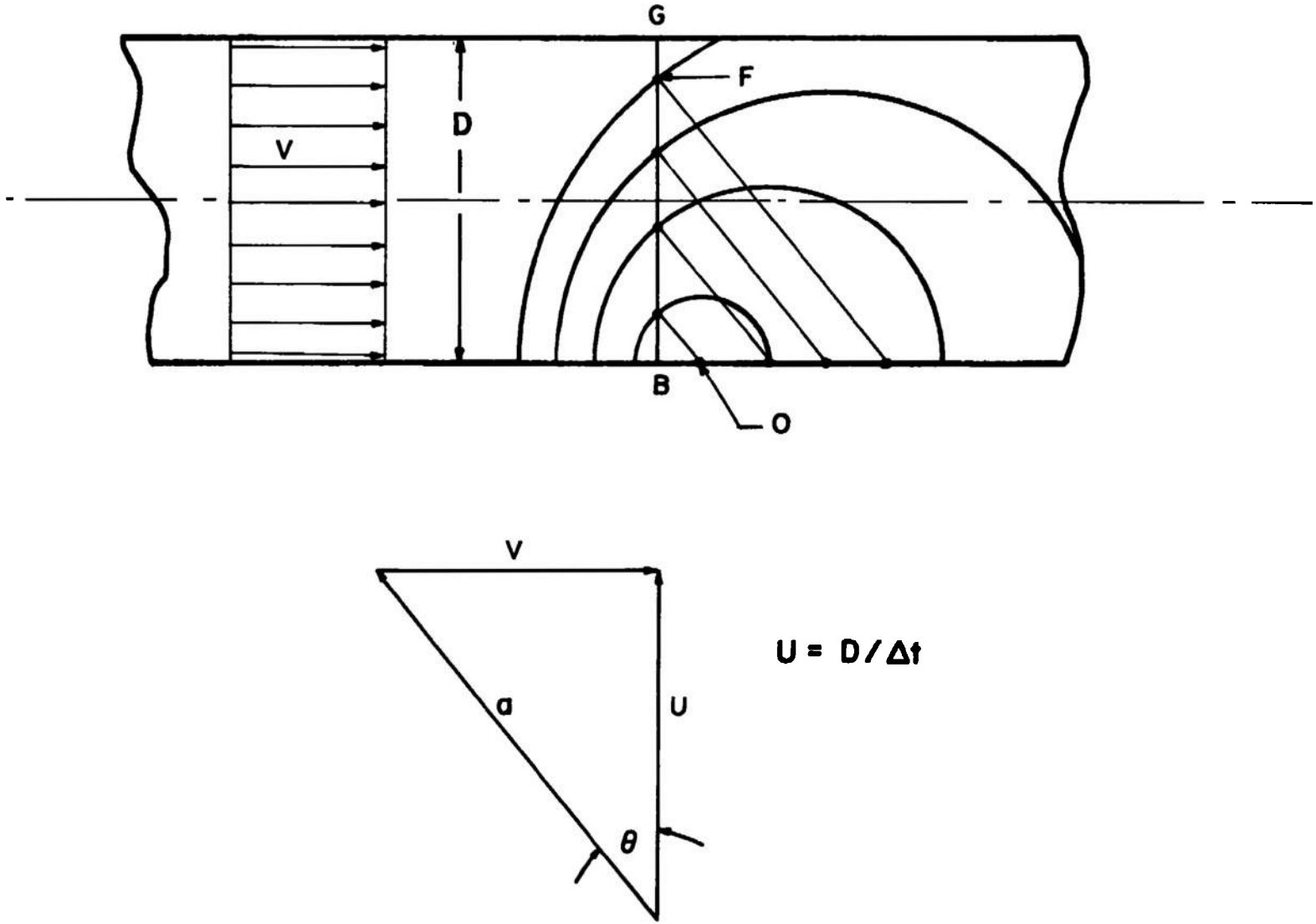

Fig. 1 Acoustic Flow Model

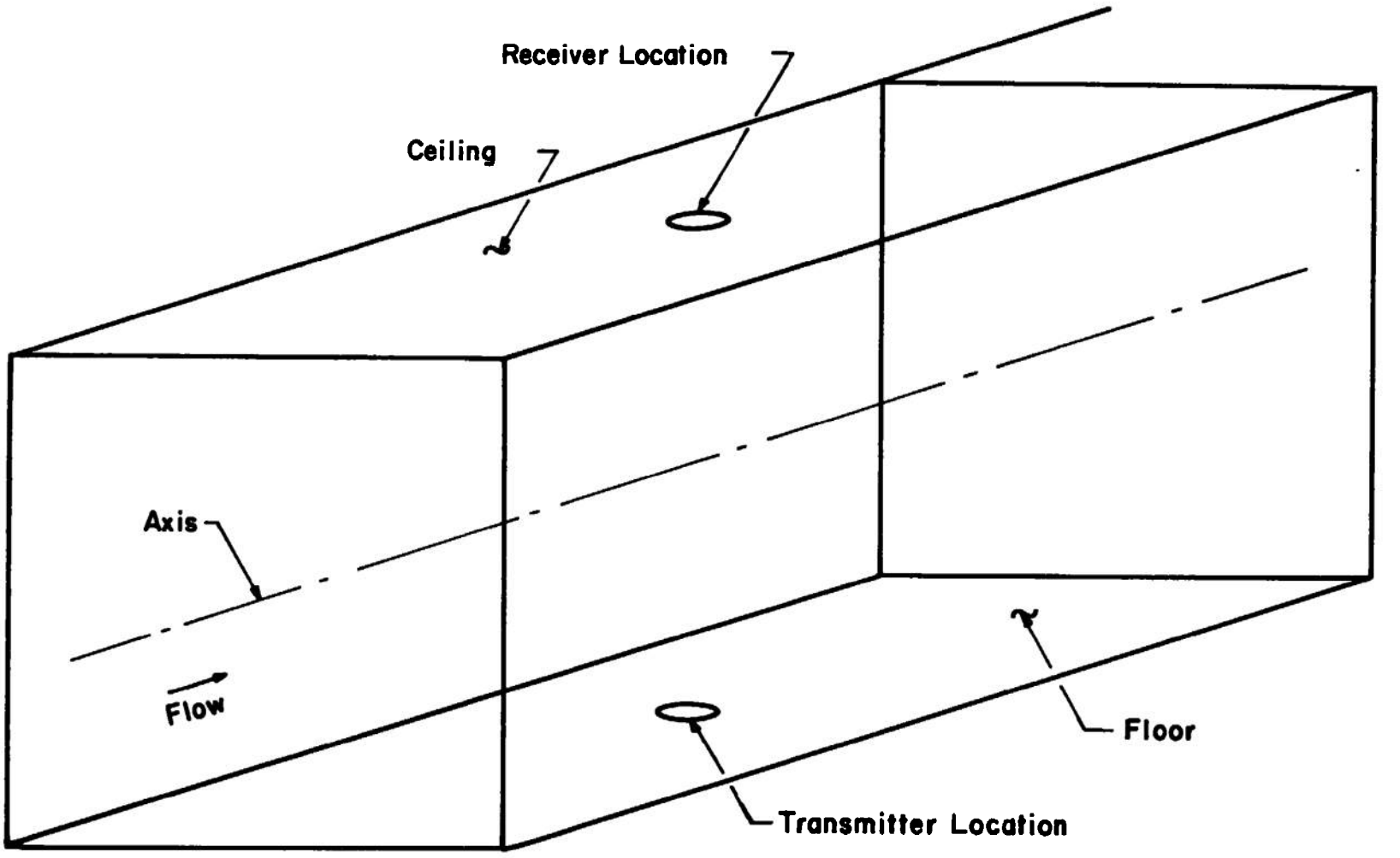

Fig. 2 Line Isometric, Test Section, Tunnel 1T

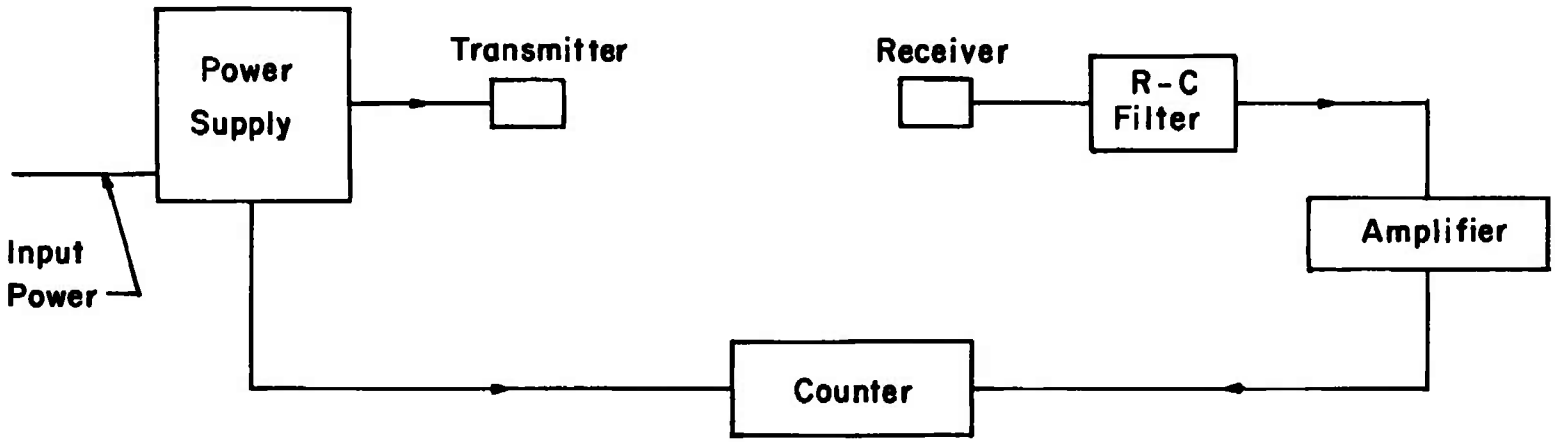

Fig. 3 Acoustic System, Basic Circuitry

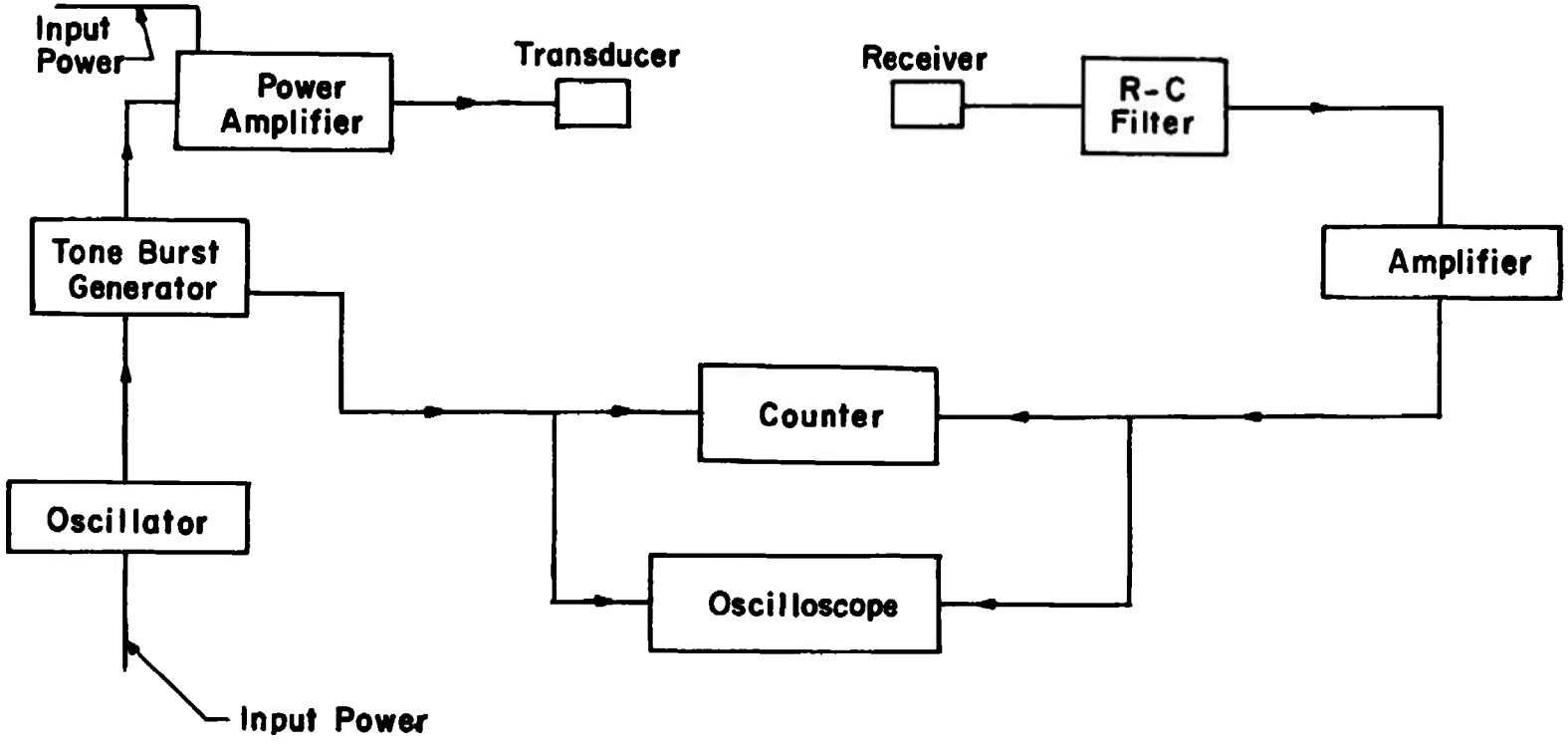

Fig. 5 Acoustic System, Transducer Circuitry

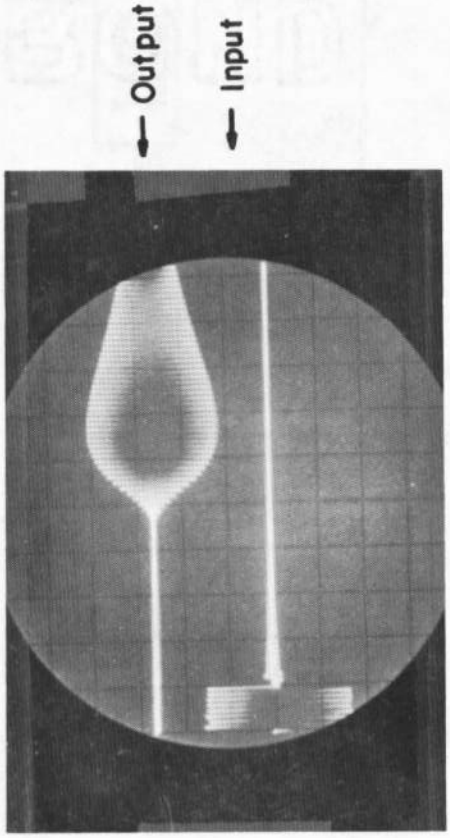

Fig. 4 Response, Pulsed Transducer

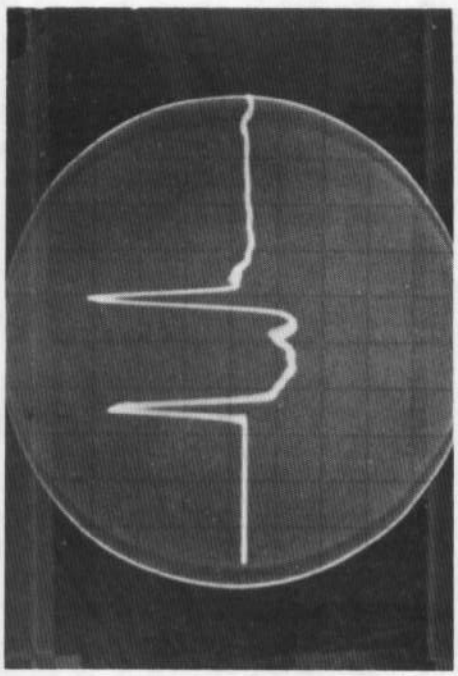

Fig. 6 Response, Arc-Gap

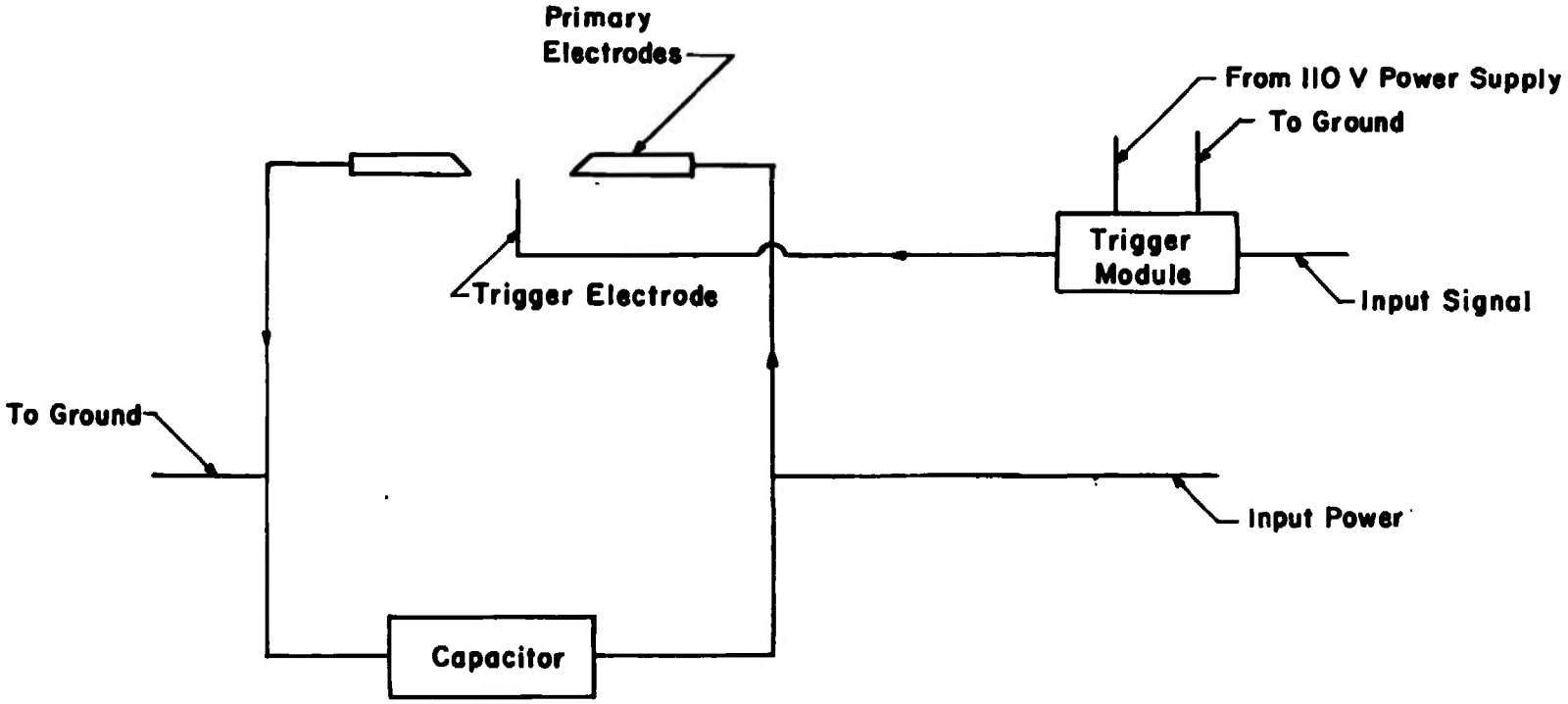

Fig. 7 Schematic, Arc-Gap

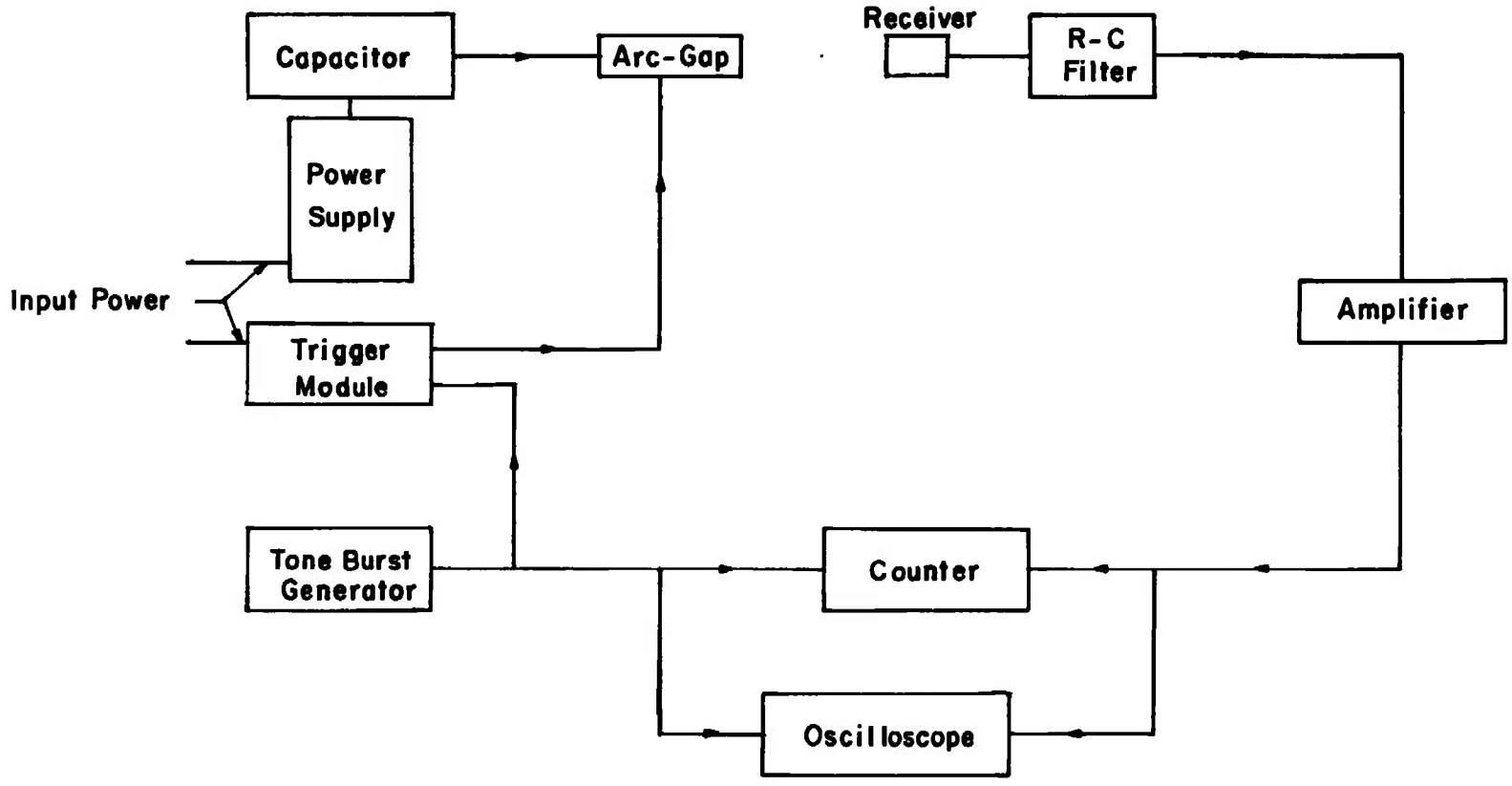

Fig. 8 Acoustic System, Arc-Gap Circuitry

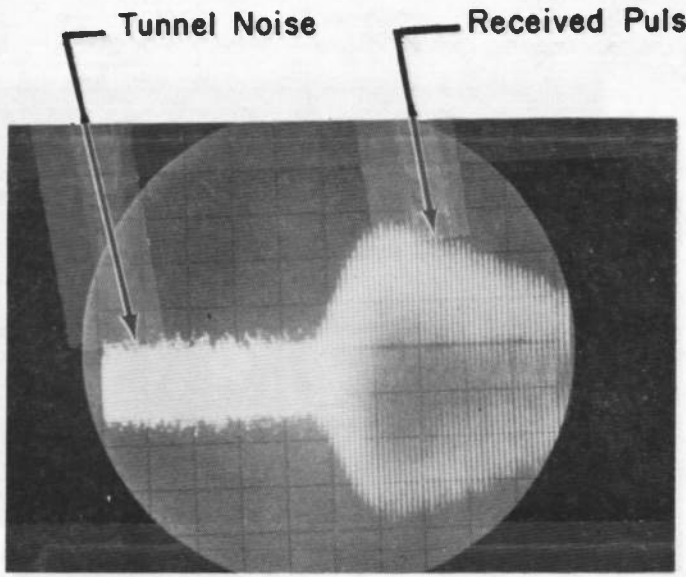

Fig. 9 Receiver Output, Pulsed Transducer, with Tunnel Flow

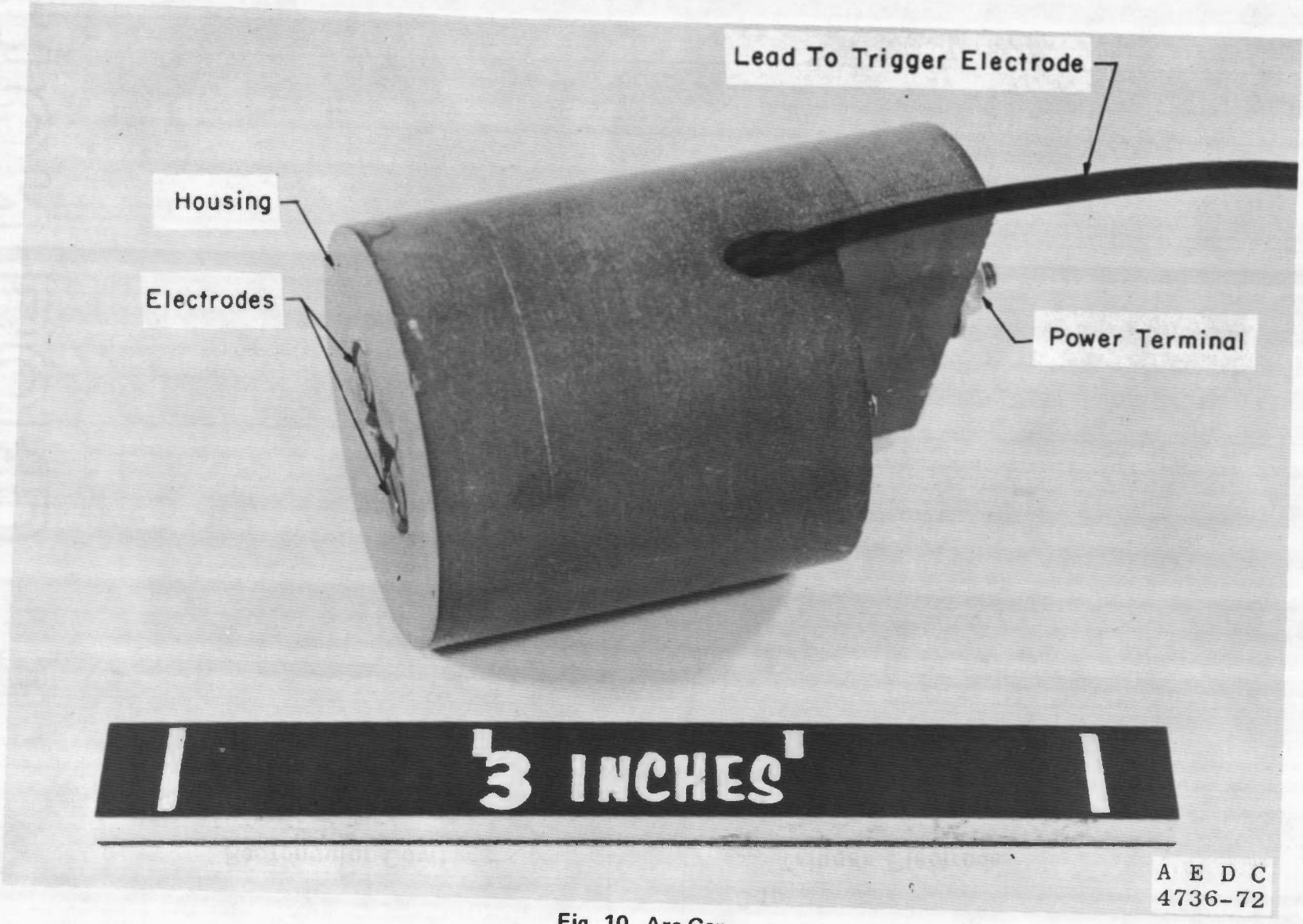

Fig. 10 Arc-Gap

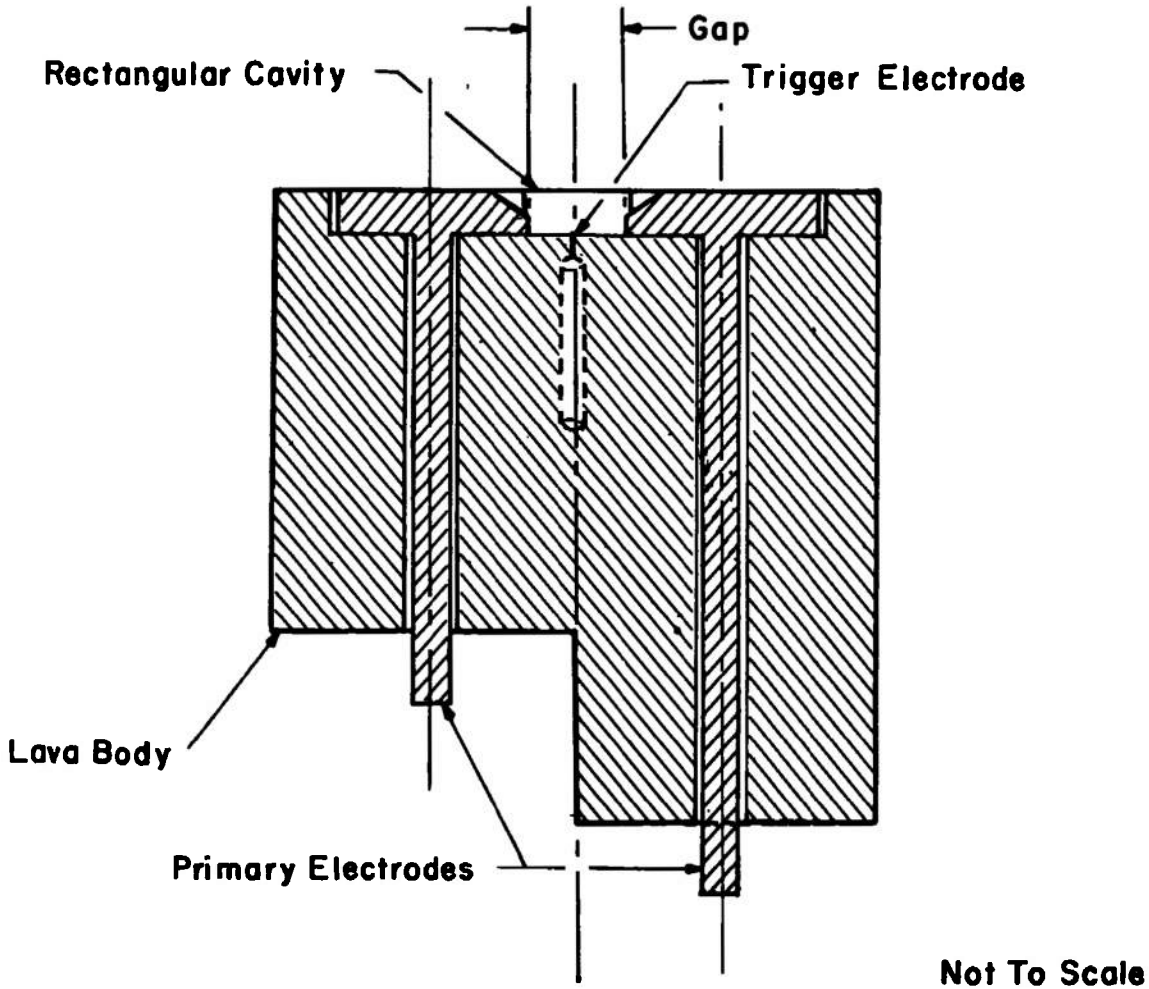

Fig. 11 Cross-Section, Arc-Gap

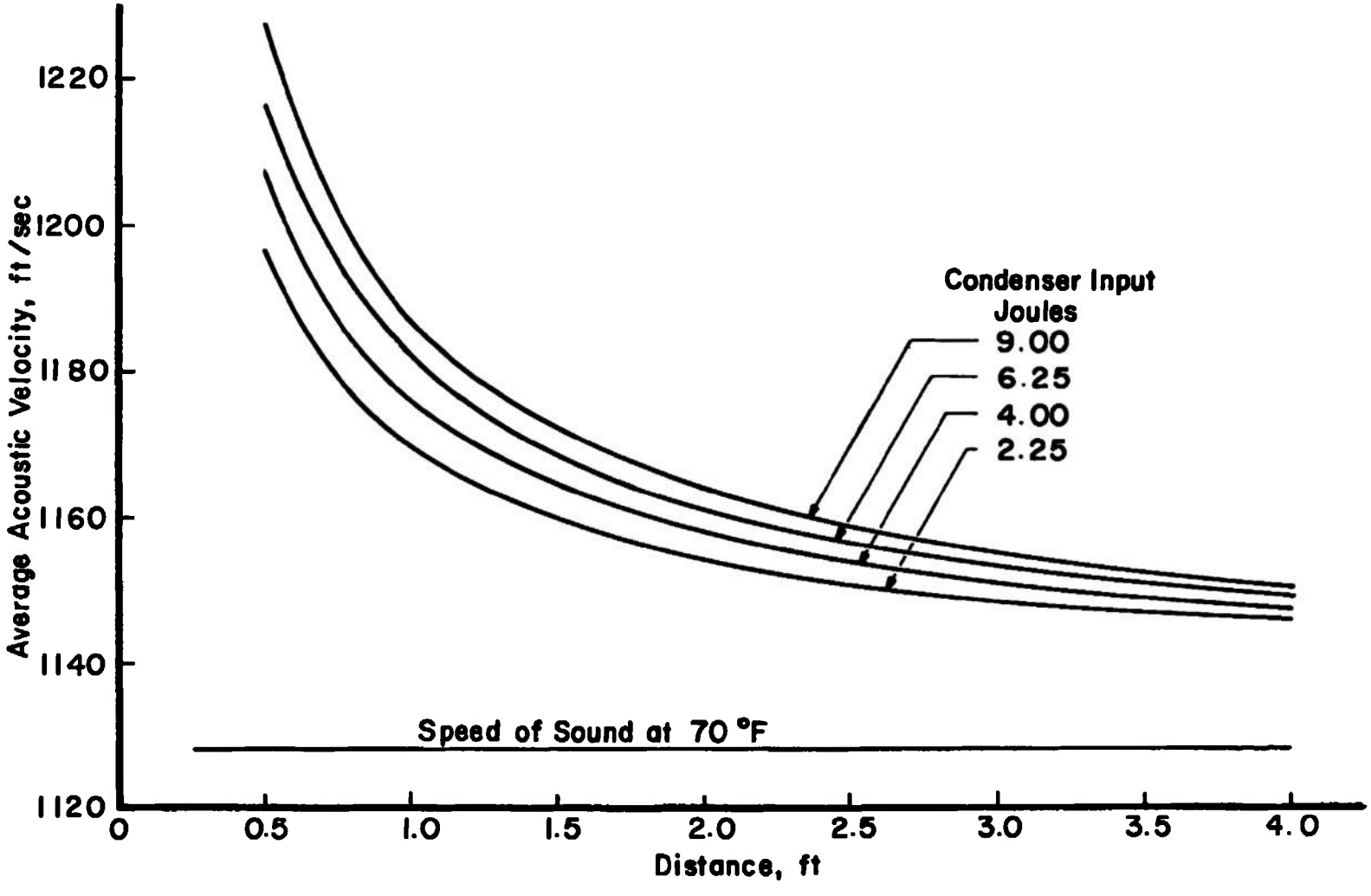

Fig. 12 Calibration, Average Wave Velocity, Arc-Gap with 2.0-μf Condenser

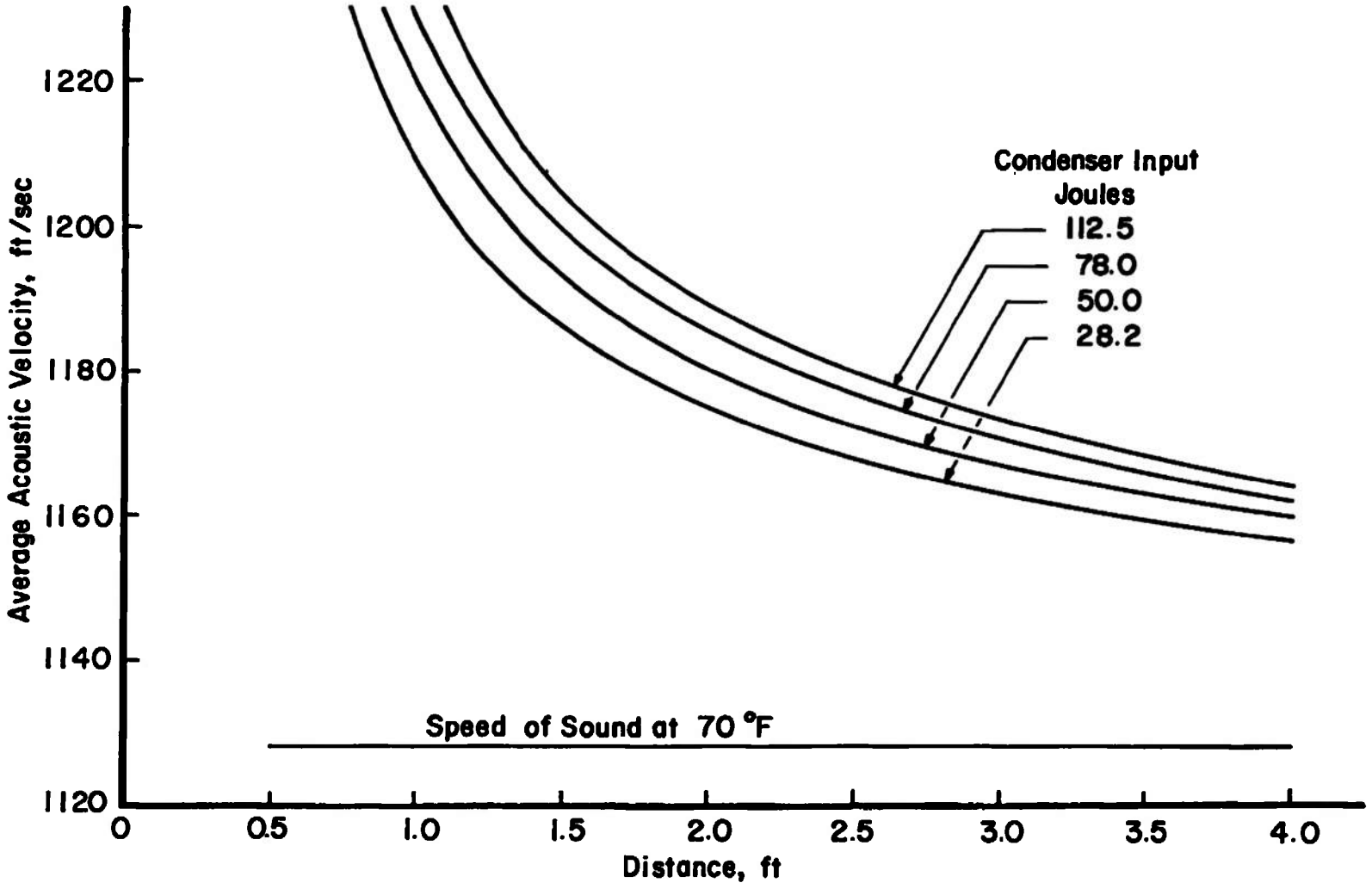

Fig. 13 Calibration, Average Wave Velocity, Arc-Gap with 25.0-μf Condenser

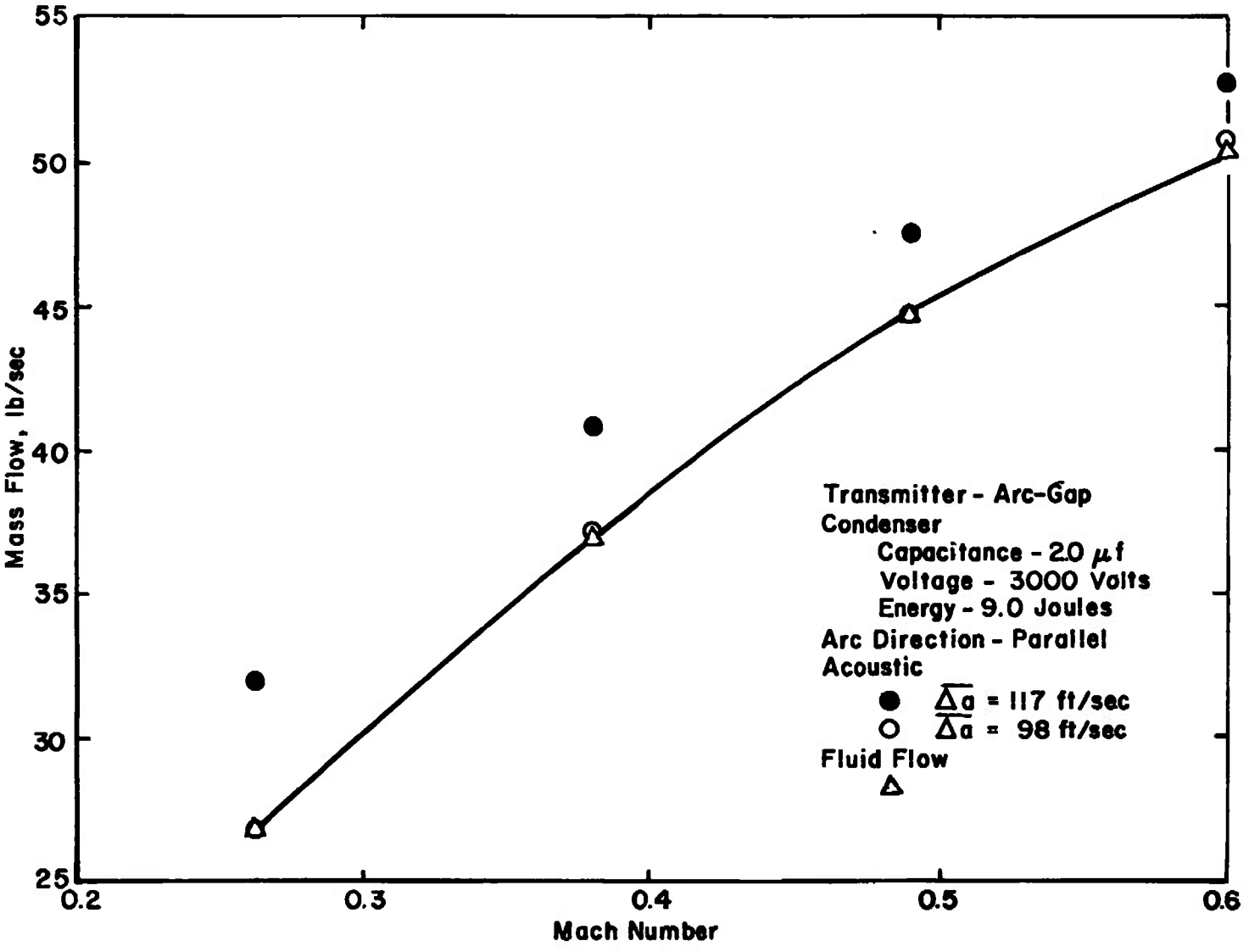

Fig. 14 Mass Flow for $\overline{\Delta a}$ of 98.0 ft/sec and Parallel Arc Direction

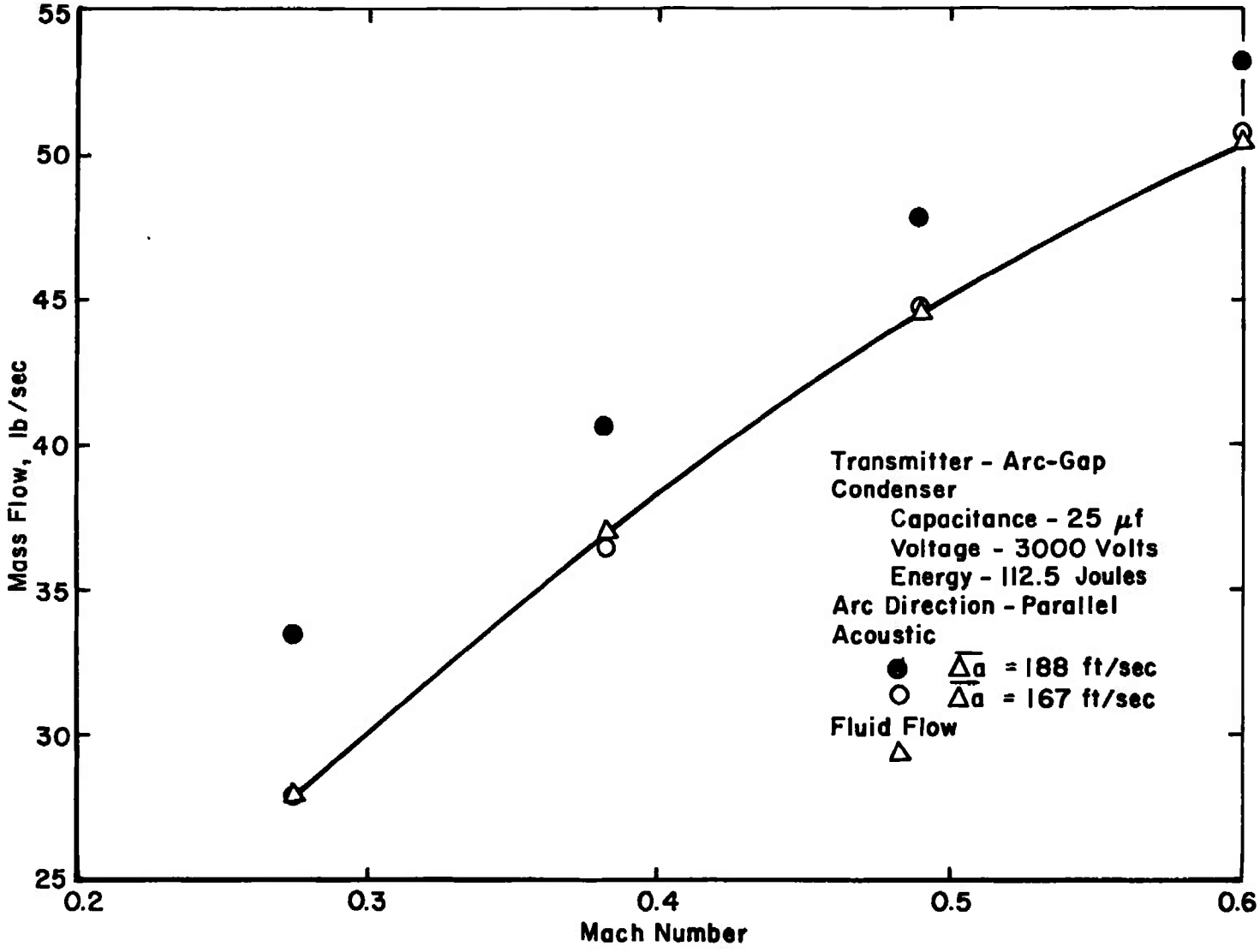

Fig. 15 Mass Flow for Δa of 167.0 ft/sec and Parallel Arc Direction

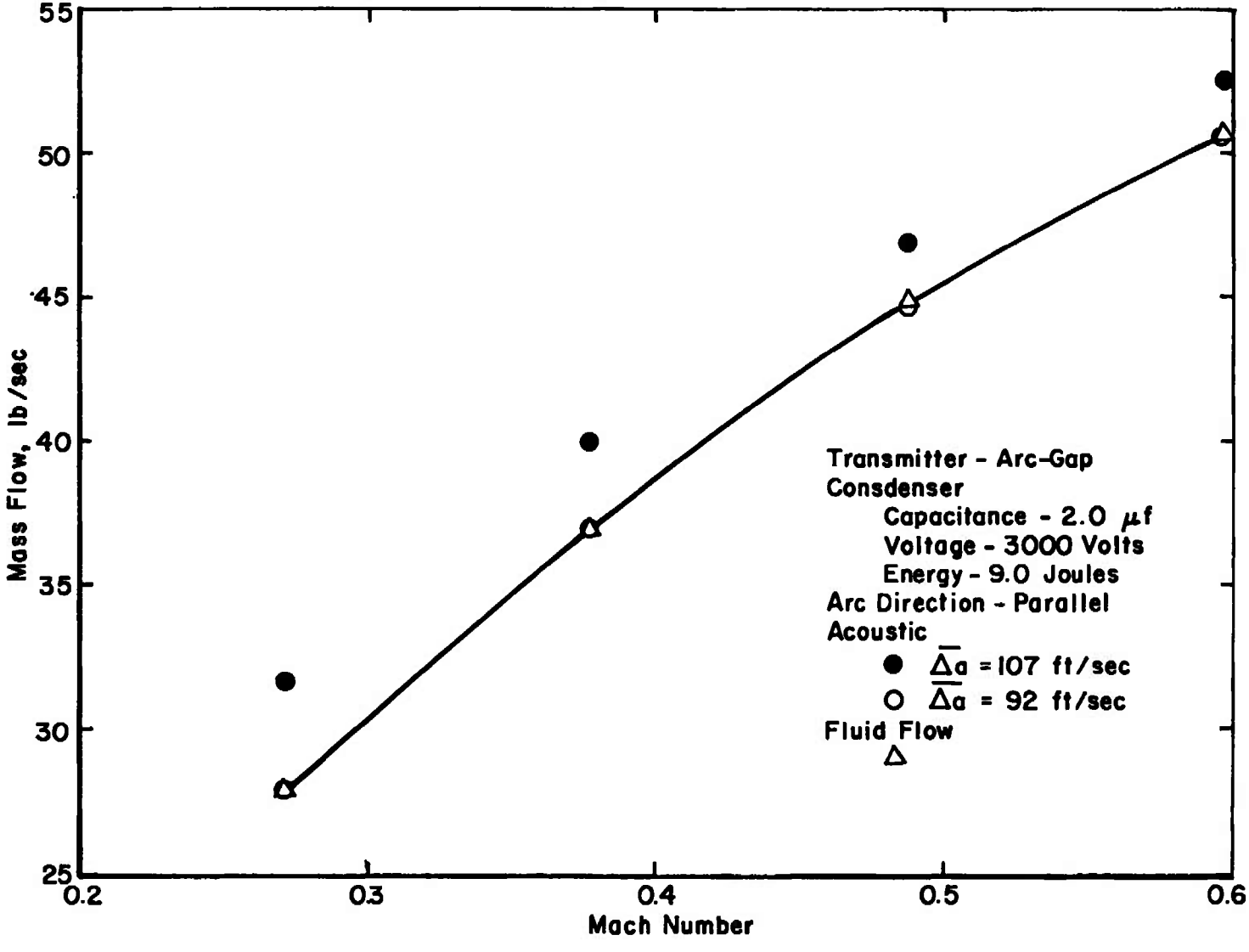

Fig. 16 Mass Flow for $\overline{\Delta a}$ of 92.0 ft/sec and Parallel Arc Direction

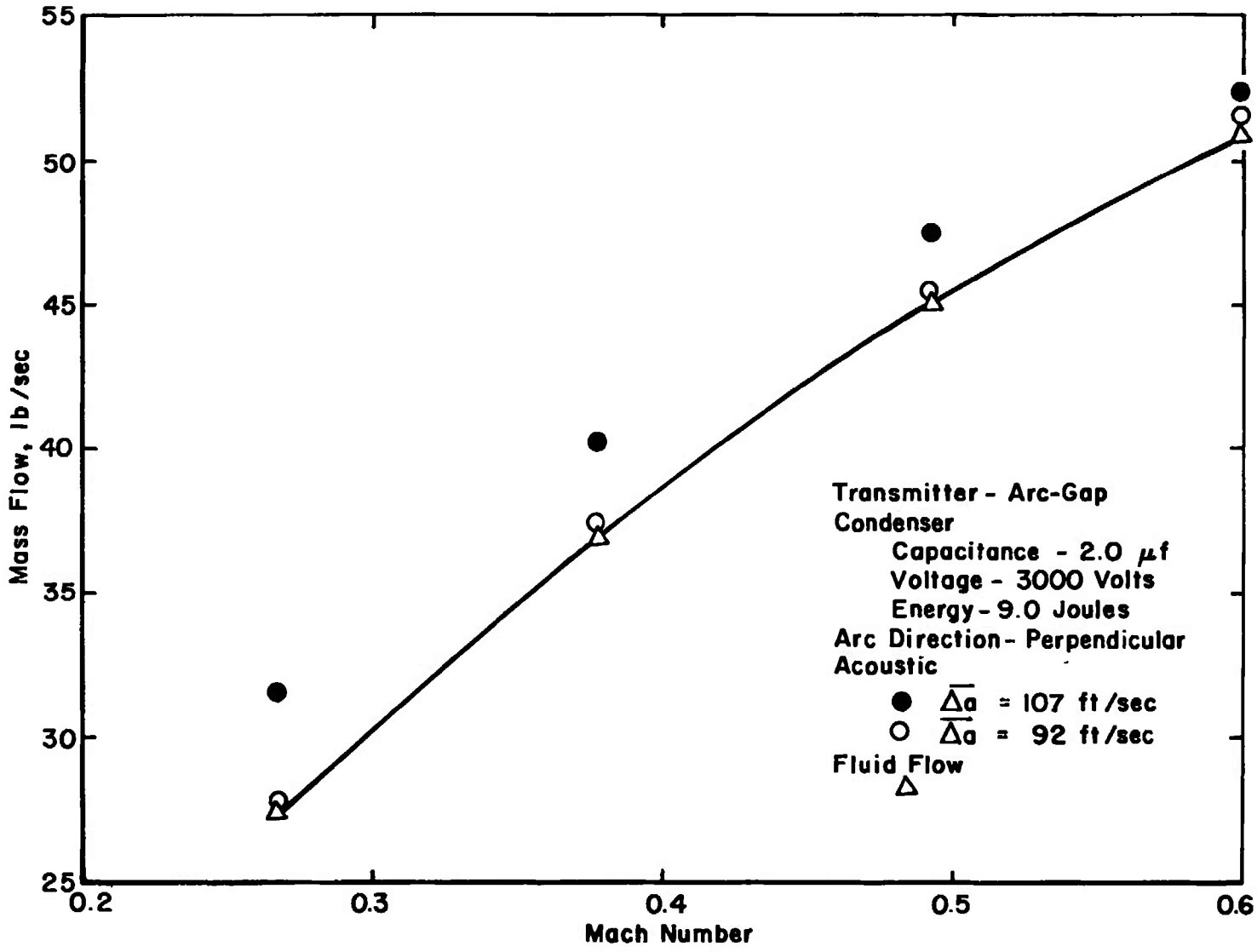

Fig. 17 Mass Flow for $\overline{\Delta a}$ of 92.0 ft/sec and Perpendicular Arc Direction

TABLE I
MAJOR COMPONENTS, ACOUSTIC SYSTEM, TRANSDUCER CIRCUITRY

Component	Manufacturer	Model No.
Receiver	B and K Instrument Co.	4138
Amplifier	Preston Scientific, Inc.	8300 XWB Model A
Counter	Hewlett-Packard	5233L
Oscilloscope	Hewlett-Packard	141A
Transducer	MASA	89G 89G
Power Amplifier	Bogen	JX30
Tone Burst Generator	Generator Radio	1396B
Oscillator	Hewlett-Packard	200CD

TABLE II
MAJOR COMPONENTS, ACOUSTIC SYSTEM, ARC-GAP TRANSMITTER CIRCUITRY

Component	Manufacturer	Model No.
Receiver	B and K Instrument Co.	4138
Amplifier	Preston Scientific, Inc.	8300 XWB Model A
Counter	Hewlett-Packard	5233L
Oscilloscope	Hewlett-Packard	141A
Trigger Module	EG & G	TM-11
Tone Burst Generator	Generator Radio	1396B

APPENDIX III
TIME OF TRAVEL MEASUREMENT

The acoustic method of this report for measuring mass flow is based on the measurement of the time of travel of an acoustic signal over a known distance between a transmitter and a receiver. This Appendix describes the manner in which the time of travel was obtained with regard to the measured time interval and corrections.

The measuring instrument was an electronic counter which includes triggering circuits to start and stop the counter with successive input signals. Input signals are voltage pulses, and the triggering circuits are activated when the rising input voltage reaches the value of the triggering voltage. Each triggering circuit includes a manual adjustment with which the triggering voltage can be set to any value between zero and the maximum value. Thus, when the maximum value of the input voltage is less than the set triggering voltage (set point), the triggering circuit will not respond. The output of the receiver includes acoustic noise in addition to the signal, and assuming a signal-to-noise ratio greater than unity, the set point adjustment is used to prevent noise interference. The set point voltage is adjusted to a value greater than the maximum noise component in the receiver output but less than the maximum value of the acoustic signal, and the triggering circuit then responds only to the acoustic signal to stop the counter. The starting triggering circuit is activated by the synchronizing pulse from the tone burst generator as previously mentioned, but that pulse does not include acoustic noise components and electrical noise is essentially nil.

The sequence of events is illustrated by Fig. III-1 in which the synchronizing pulse and the acoustic signal pulse are shown on a time base. The counter is started at time t_o when the rising voltage of the synchronizing pulse equals the set point as shown. However, the leading edge of the synchronizing pulse arrives at time t_o preceding time t_o by an interval Δt_f which is related to the slope of the forward face of the pulse. As previously mentioned, the rise time of the synchronizing pulse from zero to peak voltage is 2.0 μsec, which is indicated as Δt_s in Fig. III-1. The value of the time interval Δt_f is therefore equal to

$$\Delta t_f = \Delta t_s(E_{sp}/E_s) \qquad \text{(III-1)}$$

where

E_{sp} = set point voltage

E_s = synchronizing pulse peak voltage

The counter is stopped by the arrival of the acoustic signal pulse from the receiver when the rising signal voltage equals the set point at time t_2, and the measured time of travel is thus Δt_m. However, the leading edge of the signal pulse arrives at time t_1, and the measured time of travel includes an error Δt_g which is equal to

$$\Delta t_g = (E_{sp}/E_a)\Delta ta \qquad \text{(III-2)}$$

where

Δt_a = rise time of acoustic pulse

E_a = acoustic pulse peak voltage

As previously mentioned, the rise time of the acoustic pulse from zero to peak voltage is 2.0 μsec as measured under quiescent conditions. It can be shown that the rise time, Δt_a, increases with flow velocity as given by

$$\Delta t_a = \frac{\Delta t_a'}{[1 - M^2]} \qquad \text{(III-3)}$$

where

$\Delta t_a'$ = 2.0 μsec

M = flow Mach number

Therefore,

$$\Delta t_g = \frac{E_{sp}\,\Delta t_a'}{E_a[1 - M^2]} \qquad \text{(III-4)}$$

Although not shown in Fig. III-1, other events occur which contribute an additional error to the measured time of travel. That error is caused by transmission delay of electrical signals throughout the circuitry of the system shown in Fig. 8. The events depicted by Fig. III-1 include the assumptions that the arc-gap discharges simultaneously with

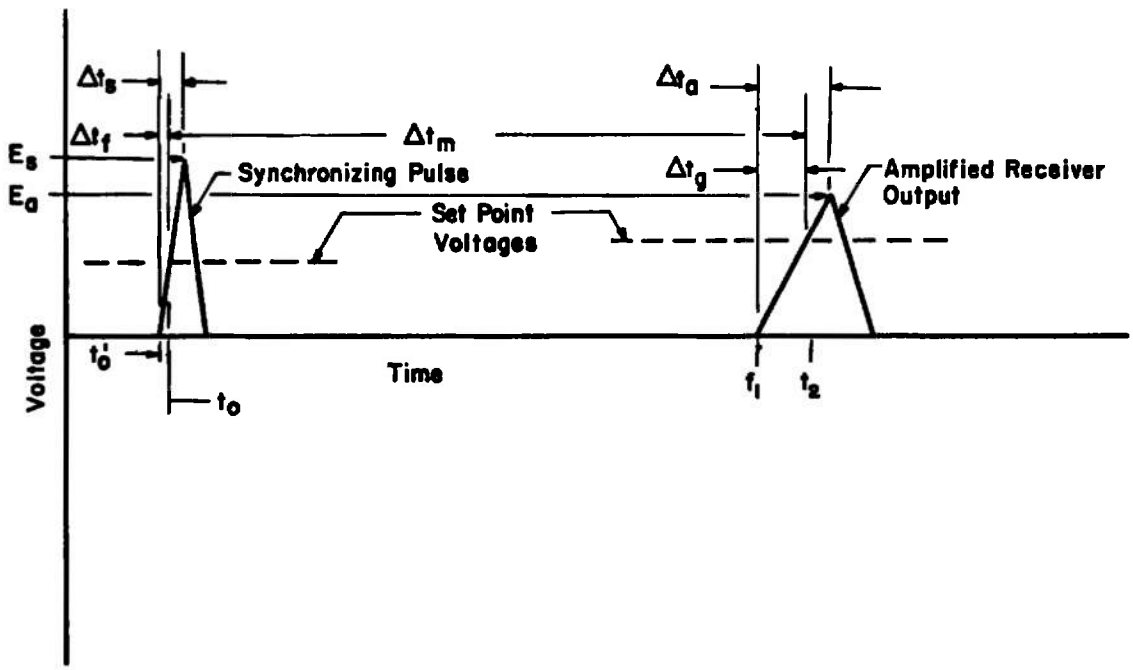

Fig. III-1 Time of Travel Sequence

the arrival at the counter of the leading edge of the synchronizing pulse at time t_o', and that the leading edge of the signal pulse arrives at the counter simultaneously with the arrival of the leading edge of the acoustic pulse at the diaphragm of the receiver at t_1. Because of transmission delays, those assumptions are not valid, and the measured time of travel includes an error from that source. The transmission delay error was measured by a technique which, in effect, placed the arc in physical contact with the diaphragm of the receiver to insure simultaneous motion of the receiver diaphragm with the discharge of the arc-gap. That arrangement eliminated Δt_f and Δt_g of Fig. III-1, and it also eliminated the time of travel between the arc-gap and the receiver. In the absence of transmission delay factors, a counter reading of zero would have been obtained on discharge of the arc-gap. Instead, a value of 22.0 μsec was recorded from numerous readings. That transmission delay error as designated and used in all computations is

$$\Delta t_d = 22.0\ \mu\text{sec} \qquad \text{(III-5)}$$

As described in Section II and in Appendix IV, the actual time of travel, Δt, of the acoustic signal from transmitter to receiver is related to the flow velocity. The actual time of travel from the preceding, is

$$\Delta t = \Delta t_m + \Delta t_f - \Delta t_g - \Delta t_d \qquad \text{(III-6)}$$

The time of travel measuring system in Fig. 8 and as used for the Tunnel 1T tests did not include provisions for measuring peak signal voltages, and therefore, the time intervals Δt_f and Δt_g as given by Eqs. (III-1) and (III-4), respectively, could be evaluated. However, the maximum possible value of Δt_f was 2.0 μsec, as previously mentioned, and its contribution to Δt, Eq. (III-6), would be negligible in any case; time of travel values in Tunnel 1T were greater than 800 μsec. Therefore, Δt_f was ignored in Eq. (III-6). The maximum possible values of Δt_g were 2.0 μsec for a tunnel Mach number of 0 and 4.0 μsec at the highest test Mach number of 0.7. In the application of Eq. (III-6) in data reduction, a value of 2.0 μsec for Δt_g was used throughout, and this introduced a corresponding error in the actual time of travel from Eq. (III-6) of 1.0 μsec or less.

It should be noted that instrumentation for measuring peak voltages and the set point voltage for use in Eqs. (III-1) and (III-4) was not provided because the project objective to demonstrate feasibility did not require the relatively small improvement in accuracy. From a technical point of view, those parameters can be measured and the inclusion of the necessary instrumentation in another system would present no problems.

APPENDIX IV
ANALYTICAL PROCEDURES

The analytical model of Section II was based on the assumption that the wave velocity was equal to the temperature dependent sonic velocity. Results of the bench tests showed that the wave velocity is significantly greater because of the overpressure effect of the high energy arc discharge. The analysis for mass flow with the overpressure effect is given in this Appendix. Equations for computing mass flow from tunnel pressure and temperature data on the basis of fluid flow are also given.

ACOUSTIC METHOD

From the vector diagram of Fig. 1, and replacing a by $\bar{a}_w$ and U by $\overline{U}$

$$V^2 = \bar{a}_w^2 - \overline{U}^2 \tag{IV-1}$$

where

$$\bar{a}_w = a + \overline{\Delta a} \tag{IV-2}$$

$$a = (gkRT)^{1/2} \tag{IV-3}$$

$$\overline{\Delta a} = \text{average wave velocity increment} \tag{IV-4}$$

$$\overline{U} = (D/\Delta t), \text{ average signal velocity} \tag{IV-5}$$

Combining Eqs. (IV-1) and (IV-2)

$$V^2 = (a + \overline{\Delta a})^2 - \overline{U}^2 \tag{IV-6}$$

$$V^2 = a^2 + 2a\overline{\Delta a} + \overline{\Delta a}^2 - \overline{U}^2 \tag{IV-7}$$

From the energy equation

$$T = T_t \left[1 - \left(\frac{k-1}{2}\right) \frac{V^2}{a_t^2}\right] \tag{IV-8}$$

where

$$a_t^2 = gkRT_t \tag{IV-9}$$

From Eqs. (IV-3) and (IV-8)

$$a^2 = a_t^2\left[1 - \left(\frac{k-1}{2}\right)\frac{V^2}{a_t^2}\right] \tag{IV-10}$$

Combining Eqs. (IV-7) and (IV-10)

$$V^2 = a_t^2\left[1 - \left(\frac{k-1}{2}\right)\frac{V^2}{a_t^2}\right] + 2a_t\left[1 - \left(\frac{k-1}{2}\right)\frac{V^2}{a_t^2}\right]^{1/2}\overline{\Delta a} + \overline{\Delta a}^2 - \overline{U}^2 \tag{IV-11}$$

Defining a function

$$G^2 = \left[1 - \left(\frac{k-1}{2}\right)\frac{V^2}{a_t^2}\right] \tag{IV-12}$$

From Eq. (IV-12)

$$V^2 = \left(\frac{2a_t^2}{k-1}\right)[1 - G^2] \tag{IV-13}$$

Substituting Eqs. (IV-12) and (IV-13) into Eq. (IV-11)

$$\left(\frac{2a_t^2}{k-1}\right)[1 - G^2] = a_t^2 G^2 + 2a_t\overline{\Delta a}\,G + \overline{\Delta a}^2 - U^2 \tag{IV-14}$$

$$a_t^2\left[1 + \left(\frac{2}{k-1}\right)\right]G^2 + 2a_t\overline{\Delta a}G + \overline{\Delta a}^2 - \overline{U}^2 - \left(\frac{2a_t^2}{k-1}\right) = 0 \tag{IV-15}$$

$$G^2 + 2\left(\frac{k-1}{k+1}\right)\left(\frac{\overline{\Delta a}}{a_t}\right)G + \left(\frac{k-1}{k+1}\right)\left(\frac{\overline{\Delta a}^2 - \overline{U}^2}{a_t^2}\right) - \left(\frac{2}{k+1}\right) = 0 \tag{IV-16}$$

Solving Eq. (IV-16) as a quadratic in G

$$G = -\left(\frac{k-1}{k+1}\right)\left(\frac{\overline{\Delta a}}{a_t}\right) \pm \left[-2\,\frac{(k-1)}{(k+1)^2}\left(\frac{\overline{\Delta a}}{a_t}\right)^2 + \left(\frac{k-1}{k+1}\right)\left(\frac{U}{a_t}\right)^2 + \left(\frac{2}{k+1}\right)\right]^{1/2} \tag{IV-17a}$$

The radical term in Eq. (IV-17) may be given either positive or negative signs. However, it can be shown that only the positive sign is valid. Therefore,

$$G = -\left(\frac{k-1}{k+1}\right)\left(\frac{\overline{\Delta a}}{a_t}\right) + \left[-2\frac{(k-1)}{(k+1)^2}\left(\frac{\overline{\Delta a}}{a_t}\right)^2 + \left(\frac{k-1}{k+1}\right)\left(\frac{\bar{U}}{a_t}\right)^2 + \left(\frac{2}{k+1}\right)\right]^{1/2} \quad \text{(IV-17b)}$$

Substituting Eqs. (IV-17) in (IV-13)

$$V^2 = \left(\frac{2a_t^2}{k-1}\right)\left[1 - \left(-\left(\frac{k-1}{k+1}\right)\left(\frac{\overline{\Delta a}}{a_t}\right) + \left[-2\frac{(k-1)}{(k+1)^2}\left(\frac{\overline{\Delta a}}{a_t}\right)^2 + \left(\frac{k-1}{k+1}\right)\left(\frac{\bar{U}}{a_t}\right)^2 + \left(\frac{2}{k+1}\right)\right]^{1/2}\right)^2\right] \quad \text{(IV-18)}$$

and

$$V = a_t\left(\frac{2}{k-1}\right)^{1/2}\left[1 - \left(-\frac{k-1}{k-1}\frac{\overline{\Delta a}}{a_t} + \left[-2\frac{(k-1)}{(k+1)^2}\left(\frac{\overline{\Delta a}}{a_t}\right)^2 + \frac{k-1}{k+1}\left(\frac{\bar{U}}{a_t}\right)^2 + \left(\frac{2}{k+1}\right)\right]^{1/2}\right)^2\right]^{1/2} \quad \text{(IV-19)}$$

Equation (IV-19) gives the flow velocity, as a function of the sonic velocity at total temperature, a_t, the average wave velocity increment, $\Delta\bar{a}$, and the average signal velocity, $\bar{U}$. Mass flow is given by

$$m = VAd \quad \text{(IV-20)}$$

where

$$\begin{aligned} d &= P/RT \\ A &= \text{flow area} \end{aligned} \quad \text{(IV-21)}$$

Therefore

$$m = \left(\frac{VAP}{RT}\right) \quad \text{(IV-22)}$$

and since [Eq. (IV-8)]

$$T = T_t\left[1 - \left(\frac{k-1}{2}\right)\frac{V^2}{a_t^2}\right]$$

then

$$m = \frac{[VAP]}{RT_t\left[1-\left(\frac{k-1}{2}\right)\frac{V^2}{a_t^2}\right]} \tag{IV-23}$$

or

$$m = \frac{[a_t^2][VAP]}{[RT_t]\left[a_t^2-\left(\frac{k-1}{2}\right)V^2\right]} \tag{IV-24}$$

Substituting Eq. (IV-9) into Eq. (IV-24) for a_t^2,

$$m = \frac{[gk\ \ VAP]}{\left[gkRT_t-\frac{(k-1)}{2}\ V^2\right]} \tag{IV-25}$$

The mass flow is obtained from Eq. (IV-25) in conjunction with Eqs. (IV-5), (IV-18), and (IV-19).

FLUID FLOW METHOD

The mass flow computed from fluid flow data is given by [Eq. (IV-22)]

$$m = \left(\frac{VAP}{RT}\right)$$

Since [Eq. (IV-8)]

$$\frac{T}{T_t} = \left[1-\left(\frac{k-1}{2}\right)\left(\frac{V}{a_t}\right)^2\right]$$

Assuming isentropic expansion

$$V^2 = \left(\frac{2a_t^2}{k-1}\right)\left[1-\frac{T}{T_t}\right] \tag{IV-26}$$

$$\frac{T}{T_t} = \left(\frac{P}{P_t}\right)^{\frac{k-1}{k}} \tag{IV-27}$$

Combining Eqs. (IV-26) and (IV-27)

$$V^2 = \frac{2a_t^2}{k-1}\left[1-\left(\frac{P}{P_t}\right)^{\frac{k-1}{k}}\right] \tag{IV-28}$$

$$V = a_t\left(\frac{2}{k-1}\right)^{\frac{1}{2}}\left[1-\left(\frac{P}{P_t}\right)^{\frac{k-1}{k}}\right]^{\frac{1}{2}} \tag{IV-29}$$

Substituting Eqs. (IV-27) and (IV-29) into Eq. (IV-22),

$$m = \frac{AP\,a_t\left[\frac{2}{k-1}\right]^{\frac{1}{2}}\left[1-\left(\frac{P}{P_t}\right)^{\frac{k-1}{k}}\right]^{\frac{1}{2}}}{RT_t\left[\frac{P}{P_t}\right]^{\frac{k-1}{k}}} \tag{IV-30}$$

UNCLASSIFIED

Security Classification

DOCUMENT CONTROL DATA - R & D

(Security classification of title, body of abstract and indexing annotation must be entered when the overall report is classified)

1 ORIGINATING ACTIVITY *(Corporate author)*
Arnold Engineering Development Center
Arnold Air Force Station, Tennessee 37389

2a. REPORT SECURITY CLASSIFICATION
UNCLASSIFIED

2b. GROUP
N/A

3 REPORT TITLE
AN EXPERIMENTAL INVESTIGATION OF AN ACOUSTIC METHOD FOR MEASURING GAS MASS FLOW

4 DESCRIPTIVE NOTES *(Type of report and inclusive dates)*
Final Report - July 1971 to July 1972

5 AUTHOR(S) *(First name, middle initial, last name)*
L. J. David and T. L. Giltinan, ARO, Inc.

6 REPORT DATE	7a. TOTAL NO. OF PAGES	7b. NO OF REFS
September 1973	58	0

8a. CONTRACT OR GRANT NO	9a. ORIGINATOR'S REPORT NUMBER(S)
b. PROJECT NO	AEDC-TR-73-140
c. Program Element 65802F	9b. OTHER REPORT NO(S) *(Any other numbers that may be assigned this report)*
d.	ARO-PWT-TR-73-5

10 DISTRIBUTION STATEMENT
Approved for public release; distribution unlimited

11 SUPPLEMENTARY NOTES	12 SPONSORING MILITARY ACTIVITY
Available in DDC	Arnold Engineering Development Center, Air Force Systems Command, Arnold AF Station, Tenn. 37389

13 ABSTRACT Airflow through the test section of a 1- by 1-ft transonic wind tunnel under subsonic flow conditions was measured by an acoustic method to evaluate the feasibility of the method. The method was based on measuring the time of travel of an acoustic signal between a transmitter and a receiver which were located on opposite walls of the tunnel on a line perpendicular to the direction of airflow. Attempts to use pulsed ultrasonic transducers were not successful because of the characteristic time constant of a pulsed transducer and because of tunnel noise. An electrical discharge arc-gap transmitter was developed which emits a signal pressure wave with an output intensity significantly greater than that of the tunnel noise. The velocity of the pressure wave is greater than the local speed of sound by an increment which arises from the overpressure caused by the arc discharge. Calibration of the wave velocity increment under quiescent conditions demonstrated very good repeatability. Correlation of mass flow obtained by the acoustic method with mass flow values obtained by considering the test section as a one-dimensional nozzle was excellent for a wave velocity increment value somewhat less than the calibrated value. The relationship between the quiescent wave velocity increment and the value required for good mass flow correlation was not found, and it remains to be defined.

DD FORM 1 NOV 65 1473

UNCLASSIFIED

Security Classification

14. KEY WORDS	LINK A		LINK B		LINK C	
	ROLE	WT	ROLE	WT	ROLE	WT
gas flow						
ducts						
measurement						
acoustic measurement						